Article type: (Perspective/Review)

Glass Transition Phenomenon for Conjugated Polymers

*Zhiyuan Qian, Zhiqiang Cao, Luke Galuska, Song Zhang, Jie Xu, Xiaodan Gu**

Zhiyuan Qian, Zhiqiang Cao, Luke Galuska, Song Zhang, Xiaodan Gu
School of Polymer Science and Engineering, Center for Optoelectronic Materials and Device,
The University of Southern Mississippi,
Hattiesburg, Mississippi, 39406, USA
Email: xiaodan.gu@usm.edu

Jie Xu

Argonne National Laboratory, Lemont, IL 60439， USA

Key words: Conjugated polymers, Glass transition temperature, Semiconducting materials, Flexible electronics.

Abstract: Conjugated polymers are emerging as promising building blocks for a broad range of modern applications including skin-like electronics, wearable optoelectronics, soft energy and sensory technologies, given that their mechanical, optical and electronic properties can be modulated by changing their chemical structures, molecular interaction, crystal structure, morphology and surface/interface. In the past three decades, the optical and electronic properties of conjugated polymers have been extensively studied, while their mechanical properties, especially the glass transition phenomenon which fundamentally represents the polymer chain dynamics, has received much less attention. Currently, there is a lack of design rules that underpin the glass transition temperature of these semi-rigid conjugated polymers, putting a constrains on rationally polymer design for flexible stretchable devices and stable polymer glass that needed for the device's long-term morphology stability. In this review article, the glass transition

phenomenon for polymers, glass transition theories and characterization techniques are first discussed. Then previous studies on the glass transition phenomenon of conjugated polymers are reviewed and a few empirical design rules are proposed to fine-tune the glass transition temperature for conjugated polymers. The review paper is finished with perspectives on current challenges and opportunities for studying the glass transition phenomena of conjugated polymers. The goal of this perspective is to draw attention to challenges and opportunity of controlling, predicting and designing polymeric semiconductors specifically to accommodate their end use.

1. Introduction

Looking back the past few decades, the signature of the 20th century is the digital revolution. We now live in the digital age that surround by various electronics: laptop, computers, displays in our daily life. The list could go on and on. Electronics left little area untouched for modern human life. This trend will not slowdown in near future. Take annual Consumer Electronics Show (CES) for example, new form of the electronic devices emerges every year to excite the consumers, such as foldable displays, augmented reality, more recently smart phones, smart appliances and self-driving cars.

Organic electronics is a unique class of electronic devices that would complement silicon-based devices, a dominant technique used in many electronic gadgets. Since the discovery of the conductivity in polymer by Heeger, MacDiarmid, and Shirakawa, organic electronics have witted tremendous progress in the past two decades, witness tremendous improvement in electronic and optical property of semiconducting polymers. With the synergistic effort from chemists, physicists and engineers, organic light emitting diode (OLED) have been commercialized (e.g. LG OLED TV), and many other organic electronics showed great promise for commercialization. For example, organic solar cells showed impressive power convert efficiency up to 17.3%,[1] and

organic thin film transistors routinely report charge carrier mobility above amorphous silicon.[2–5] Among these organic electronics, polymeric electronics have additionally unique properties. Their optoelectronic property can be systematically tuned to meet end applications together with potential self-healing capability.[6–8] Polymeric materials are generally light weight, flexible and even deformable. Thus, recently there are several research groups started to design stretchable polymer-based transistors for wearable electronics.[9–12] Despite much interest in the designing flexible/stretchable electronic devices, the glass transition phenomenon of conjugated polymers, a parameter that directly correlated to the mechanical property of a given material, has not been carefully studied.

The glass transition phenomenon in polymer has been intensively investigated in the past 50 years. Still there are many interesting questions remain unsolved, such as the molecular mechanisms for rapid changes in the dynamics near the transition point. This review does not aim to be extensively covering the glass transition in polymer, where many excellent reviews already exists.[13–22] We will limit our discussion to conjugated polymers. Conjugated polymers have unique chain architecture that consist a rigid backbone, which is responsible to delocalized electronic cloud for charge transport, and flexible alkyl sidechains for promoting their solubility. The length of the sidechains usually ranges from 4 carbons to up to 30 carbon. Thus, the conjugated polymer can be generally viewed as a comb type polymer. Those two class of polymeric materials shared many common grounds, and meantime differs drastically in many aspects.

This review article will aim to provide insights into the glass transition phenomenon for conjugated polymers, summarize previous works and provide perspectives for future research directions. The review is organized as follows. In Sec. 2, we briefly describe the glass transition phenomena for the traditional coiled polymers, including two classical models to describe the glass

transition temperature (T_g), and parameters that affect T_g. Sec. 3 presents the different experimental techniques for measureing the T_g. Sec. 4 summaries previous studies on conjugated polymers, categorized by their backbone structure. In Sec. 5, empirical design rules of T_g for conjugated polymers are discussed based on the previous sections. Sec. 6 contains the future look for the T_g of conjugated polymers.

2. Glass transition for polymers

The glass transition of non-conjugated polymer, or regular coiled polymers, has been widely investigated for several decades, but still not been fully understood. Nevertheless, the foundation laid based on the traditional coiled polymers would help us have a better understanding on the glass transition of conjugated polymers. Here, we first introduce the glass transition phenomena, then present two popular glass transition theories: free volume theory and Gibbs-DiMarzio thermodynamic theory. Then we discuss the important molecular parameters (including molecular weight, chain rigidity, etc) that affect T_g.

2.1 The glass transition phenomena

The glass transition can be viewed as indicator for the mechanical properties of polymers at a given temperature. **Figure 1a** shows a schematic representation of the temperature dependence of Young's modulus for a typical amorphous polymer, such as polystyrene. Its viscoelastic behavior falls into five regions: liquid flow, rubbery flow, rubbery plateau, leathery (or transition), and glassy, as temperature decreases.[23,24] In the leathery regime, in which the glass transition occurs, the Young's modulus can vary by serveral orders of magnitude. **Figure 1b** shows the response of dynamic shear moduli for a regiorandom poly(3-hexylthiophene) (P3HT) in the frequency space

(low frequency equivalents to high temperature), where similar magnitude of decrease in shear moduli is observed.[25] Hence, it is pivotal to study the T_g of polymers, both commodity polymers and conjugated polymers, in order to determine the proper operation temperature range for desired applications.

Besides from the intuitive description of glass transition phenomena based on their mechanical property, it can also be observed from the thermodynamic parameters, such as specific volume. **Figure 2** shows a schematic representation of the temperature dependence of specific volume for a typical amorphous polymer. Upon cooling the polymer from the liquid state, the specific volume decreases. The molecular mobility would also decrease as temperature drops, however initially the polymer is still mobile enough so that it remains in equilibrium state. As the polymer being further cooled, the mobility becomes so low that the equilibrium is no longer able to be reached on the experimental timescale (e.g. seconds). As a result, the specific volume departures from the equilibrium and the polymer goes into the glassy state. This temperature is known as T_g. Importantly, it shows kinetic dependence, i.e., the value decreases as the cooling rate (q) decreases[26–28] and does not depend on the heating rate.[16,27,29] For instance, it has been reported that for a variety of polymers, the cooling rate dependence of T_g exhibits the following relationship: $dT_g/d\log q \approx 3$ K.[13,30–32] Also, the T_g shows a pressure dependence, which increases with the pressure by 0.3 ºC/MPa.[13,33–35]

2.2 Classic theories related to the glass transition

2.2.1 Free volume theory

Historically, the concept of free volume was developed to describe the viscosity of liquids,[13,36–39] and subsequently the super-Arrhenius temperature dependence of viscosity above

T_g.[16,40] According to Doolittle,[39] the viscosity-free volume relationship can be captured by an empirical equation:

$$\ln \eta = \ln A + B\left(v - v_f\right)/v_f \quad (1)$$

where A and B are constants, v is the specific volume, v_f is the free volume, and $v_0 = v - v_f$ is the occupied volume.

In 1950, Fox and Flory suggested that the glass transition phenomenon in polymers can be related to the free volume,[38] i.e., the glass transition takes place when the free volume in the system becomes a constant and it is independent of both the molecular weight and the temperature, i.e., the iso-free volume state.[38,41]

The free volume concept was further explored by Williams, Landel and Ferry.[42] They reported an empirical equation (the WLF equation) to describe the temperature dependence of relaxation time in glass forming liquids when above T_g ($T_g + 10$ ℃ $\leq T < T_g + 100$ ℃):[30]

$$\log a_T = \log \frac{\tau(T)}{\tau(T_0)} = \frac{-C_1^0(T-T_0)}{C_2^0+T-T_0} \quad (2)$$

where a_T is known as the shift factor, C_1^0 and C_2^0 are WLF parameters, and T_0 is the reference temperature. (a_T can also be obtained as the ratio of the viscosities at two temperatures: $a_T = \frac{\eta(T)}{\eta(T_0)}$. It is an important parameter from the time-temperature superposition principle.[30] Owing to the space and scope of this perspective, the interested readers are referred to Ref [30] for detailed discussion.) Importantly, this empirical equation can be derived from the Doolittle equation (equation 1). In their derivation, the fractional free volume is defined as $f = \frac{v}{v_f}$. Therefore, the Doolittle equation is reorganized as

$$\ln \eta = \ln A + B\left(\frac{1}{f} - 1\right) \tag{3}$$

and

$$\log a_T = \log \frac{\eta(T)}{\eta(T_0)} = \frac{B}{2.303}\left(\frac{1}{f} - \frac{1}{f_0}\right) \tag{4}$$

If the temperature dependence of f satisfies the following relation:[30]

$$f = f_0 + \alpha_f (T - T_0) \tag{5}$$

where α_f is the volumetric thermal expansion coefficient of the free volume. By substituting equation 5 to equation 4, we get

$$\log a_T = -\frac{(B/2.303 f_0)(T - T_0)}{f_0/\alpha_f + T - T_0} \tag{6}$$

Hence, it has same form as the WLF equation, with $C_1^0 = B/2.303 f_0$ and $C_2^0 = f_0/\alpha_f$. William, Landel and Ferry[42] showed that when the T_g is set as the reference temperature ($T_0 = T_g$), for a large number of polymers, C_1^g and C_2^g are found to have the universal values of 17.44 and 51.6, respectively. Subsequently, if B is taken as unity, it is readily seen that $f_g = 0.025$ and $\alpha_f = 4.8 \times 10^{-4}$ °C^{-1}. The value of α_f has a good agreement with the experimental data.[42]

It has been shown that the super-Arrhenius behavior of the temperature dependence of viscosity follows the so-called Vogel-Fulcher-Tammann (VFT) equation:[43–45]

$$\eta = \eta_0 \exp\left(\frac{B}{T - T_\infty}\right) \tag{7}$$

where η_0 and B are material-dependent constants, T_∞ is the temperature at which the viscosity goes to infinite. T_∞ is also known as the Vogel temperature and is about 50 °C below the

conventional T_g.[30] Mathematically, the VFT equation is equivalent to the WLF equation with $B = 2.303C_1^0C_2^0$ and $T_\infty = T_0 - C_2^0$.[30]

We note here that the free volume concept is found to be successful in describing the responses of polymers under hydraulic pressure. Quantitative relations similar to the WLF equation has been derived. Readers are referred to Refs [13,30] for detailed discussion.

2.2.2 Gibbs-DiMarzio thermodynamic theory

Another theory to describe the glass transition phenomenon is from thermodynamic approach, which was developed by Gibbs and DiMarzio[46,47] and based on the Flory-Huggins lattice model.[48,49] They suggested that although the T_g shows kinetic dependence, there exists a true equilibrium second-order thermodynamic transition at T_2, which is the lower limit of T_g and obtained at infinitely long experimental time-scale. In their model, n_x linear polymer chains with x segments long are placed on the lattice along with n_0 holes, or vacant sites. The configurational entropy S_c is related to the number of configurations of the molecule on the lattice. As the temperature decreases, the volume of holes decreases and the chains are in favor to take the low-energy molecular conformation, which then results in a decrease in S_c. At T_2, S_c becomes zero and remains zero even being further below T_2. Therefore, it solves the Kauzmann negative configurational entropy paradox[13,46,50] (Readers are referred to Refs [13,46,50] for detailed discussion). It was found that T_2 is approximately 50 °C below the conventional T_g,[51] and often related to the Kauzmann temperature T_K and the Vogel temperature T_∞.[14] It is worth noting here that the fraction free volume derived from Gibbs-DiMarzio theory is approximately 0.025, which incidentally is comparable to the universal value obtained from WLF equation.[13,52,53]

2.3 Parameters affect T_g

In this section, we will introduce several factors that are known to influence T_g.

2.3.1 Molecular weight

With its long chain nature, the physical properties of polymers show dependence on the molecular weight. The value of T_g for linear polymers increases with the number average molecular weight M_n and becomes a constant at high M_n, which is empirically captured by the Fox-Flory equation:[38]

$$T_g(M_n) = T_g(\infty) - \frac{K}{M_n} \tag{8}$$

where $T_g(\infty)$ is the glass transition temperature for polymer with infinite molecular weight and K is a constant.

This equation can be readily obtained from free volume theory by assuming that the fraction free volume at T_g is independent of molecular weight. If the contribution of each chain end to the excess free volume is θ, then for a linear chain, the excess free volume is 2θ. With the density ρ, Avogadro's number N_A and the molecular weight M_n, the total excess free volume per unit volume is $2\theta\rho N_A/M_n$. Therefore, for a polymer with finite molecular weight M_n, to compensate the excess free volume introduced by the free chain ends, the polymer must undergo thermal contraction, i.e., be cooled down from $T_g(\infty)$ to $T_g(M_n)$,[13,22,54–56] which is

$$\frac{2\theta\rho N_A}{M_n} = \alpha_f\left[T_g(\infty) - T_g(M_n)\right] \tag{9}$$

where α_f is the volumetric thermal expansion coefficient of the free volume. Then we get

$$T_g(M_n) = T_g(\infty) - \frac{2\theta\rho N_A}{\alpha_f M_n} \tag{10}$$

which is the same form as Fox-Flory equation with $K = 2\theta\rho N_A/\alpha_f$.

It is worth mentioning here that Gibbs-DiMarzio thermodynamic theory can also describe the decrease of T_g with decreasing M_n, the derivation is much complicated, and the interested readers are referred to Refs [13,46,56–58] for details.

2.3.2 Chain rigidity

The T_g of polymers has long been recognized to be influenced by the chain rigidity (or chain stiffness), which increases as the chain becomes more rigid (or less mobile).[23,46,47,59–63] It has been shown that there are two factors contribute to the chain rigidity.[60] The first one is the backbone flexibility and relates to the ease of backbone rotation. For instance, the backbone of poly(dimethyl siloxane) (PDMS) is extremely flexible as a result of the low rotational energy barrier, which results in a T_g of -123 °C.[23,59,60] Other examples are polyethylene (PE) and polytetrafluoroethylene (PET), which have the T_g of -90 °C and -50 °C,[23,59,60] respectively. While, by inserting the bulky groups, such as the aromatic groups, to the backbone, the T_g increases due to the higher energy barrier of ….[64] For example, poly(phenylene oxide) has a T_g of 83 °C.[53]

The second contribution comes from the pendant groups, which increases the chain rigidity because of the steric hinderance effect. For example, by substituting one H atom in PE with a methyl group (-CH_3), which is polypropylene, the T_g increases from -90 °C to -20 °C; and with an even bulkier phenyl group (-C_6H_5), which is polystyrene, the T_g is further increased to 100 °C.[53] However, long alkyl pendant groups can also increase the chain flexibility by introducing more free volume and consequently lower the T_g. For example, for poly(n-alkyl methacrylates) and poly(4-alkyl styrenes), the T_g decreases as the number of carbon atoms in alkyl groups increases. (when the number of carbon is greater than 12, the T_g starts increasing again as a result of the side

chain crystallization, which then reduces the chain mobility)[65] This effect is also known as the 'internal plasticization effect'. The sidechain effect for conjugated polymers will be discussed in section 5 in more details.

2.3.3 Crystallinity

It is known that the semicrystalline polymers consist of three fractions: crystalline fraction (CF), mobile amorphous fraction (MAF), and rigid amorphous fraction (RAF).[66] The RAF is considered to be the amorphous region in the immediate vicinity of the crystalline domain, which separates the MAF from CF.[67] The chain dynamics of RAF is constraint by the immobile CF, while the chain dynamics of MAF is independent of CF. Therefore, a separated T_g for RAF, higher that the T_g for MAF, is expected. This has been observed in a variety of regular semicrystalline polymers,[66] and recently in a conjugated polymer poly(3-hexylthiophene) (P3HT)[68] as well.

2.3.4 Nanoconfinement effect

The nanoconfinement effect has a strong influence on the T_g. Inspired by the pioneering work of Jackson and McKenna on the T_g depression for the organic liquids confined in nanopores,[69] the T_g of polymers in the nanometer scales has received significant interest.[19–21,34,70–80] The Tg of thin films, a simplest nanoconfined physical model, has been characterized by different types of measurements, including dynamic,[81–85] thermodynamic[86,87] and pseudo-thermodynamic[75,88–98] (see subsequently for the definitions[34]). In addition, it can also be obtained by investigating the thin film rheological behavior.[99–109]

In general, for the free-standing films, because of the free surface effect, the T_g decreases with film thickness.[79] Forrest and co-workers reported a dramatic depression of 60~80 °C in T_g for free-standing polystyrene (PS) thin film at the thickness of approximately 40 nm measured with

Brillouin light scattering and ellipsometry;[92–94] McKenna and coworkers also observed the depression in T_g for free-standing PS film[110,111] using the nanobubble inflation technique,[108,109] but the magnitude is slightly smaller at the same thickness region. Moreover, with the same technique, a reduction of as much as 120 °C in T_g was reported for a 3 nm polycarbonate (PC) thin film by McKenna and co-workers.[112] It is worth noting here that the magnitude of T_g reduction varies with the chemical structure, for instance, compared with PS, polymethyl methacrylate (PMMA) shows a less pronounced T_g reduction of approximately 10 °C at the thickness of 40 nm region.[113,114] In the case of the supported film, depends on the interaction between substrate and polymer thin film, mix results of changing in T_g (decrease, increase or no change) have been reported.[79,88,115] For the supported PMMA thin film, Keddie et al.[88] observed an increase in T_g on the native oxide of silicon and a decrease in T_g evaporated gold. In addition, for the free-standing film, the T_g exhibits a dependence on the molecular weight,[93,94] whereas for the supported film, it shows no molecular weight dependence.[75,93,115]

2.3.5 Other factors

In addition to the factors discussed above, the T_g of polymers is found to be influenced by other factors, including the intermolecular coupling (e.g. H-bonding, crosslinking), tacticity, pressure, etc. In general, the T_g of a polymer decreases with the increase of the chain mobility or free volume. For example, the crosslinkers introduced to a polymer reduce the chain mobility and subsequently increase the T_g. And same argument can be applied to the hydrogen bonds, which are act as the physical crosslinkers.

3 Experimental techniques to measure T_g

The T_g of polymers, both in bulk and nanoscale, can be measured with different experimental techniques which are generally fall into three categories: dynamic, thermodynamic and pseudo-thermodynamic.

According to Alcoutlabi and McKenna,[34] the dynamic measurements obtain the T_g by investigating the temperature dependence of the relaxation time, viscosity etc.; the thermodynamic measurements directly measure the thermodynamic property (e.g., volume or heat capacity) as a function of temperature; in the pseudo-thermodynamic measurements, the property (e.g., film thickness, Brillouin frequency etc.) which is related to the thermodynamic property is investigated as a function of temperature. Here, several common measurements for T_g characterization for both traditional polymers and conjugated polymers are briefly described. The methods are catalogued, to the best of our knowledge, based on the above definition.

3.2 Dynamic measurements

3.2.1 Broadband dielectric spectroscopy

Broadband dielectric spectroscopy (BDS) has been widely used to study the dynamics of glass forming systems, including polymers. Normally, the complex dielectric permittivity ε^* of a material subjected to an electric field is measured, with $\varepsilon^* = \varepsilon' - i\varepsilon''$, ε' and ε'' are real part (or dielectric constant) and imaginary part (or dielectric loss) of ε^*, respectively. The measurement can be performed as a function of frequency f at different isotherms or as a function of temperature at a fixed frequency f.[116] The frequency range of BDS covers 18 decades, from 10^{-6} to 10^{12} Hz,[116,117] which has the capability to detect multiple relaxation processes, including the glass transition (also known as the α relaxation) and sub-T_g relaxations. The common practice of measuring T_g is by performing the frequency sweep at different isotherms. A peak corresponding to the α relaxation is observed in the dielectric loss response. The α relaxation time τ_α at each temperature can be determined by fitting the dielectric response with Havriliak-Negami equation,[117,118] which can be described by the VFT[43–45] (or WLF[42]) equation and T_g is normally defined as the temperature at which the τ_α equals to 100 seconds.[117] In addition to the bulk measurement, BDS can also be used to measure the T_g for polymer thin films with nanometer size

scale.[81–85] However, BDS technique is sensitive to the conductivity of the material. For material has electric conductivity, the low-frequency conductivity slope can mask the dielectric relaxation response of the material, which results in the difficulties in the data analysis.[18,119,120] Hence, the application of BDS on measuring T_g for conjugated polymers is limited.[25,121–123]

3.2.2 Dynamic mechanical analysis

Dynamic mechanical analysis (DMA) is an analogous to BDS, in which the material is subjected to the mechanical oscillation rather than the electrical oscillation. In general, a dog-bone shaped sample is prepared. A temperature ramp measurement at a certain heating rate (e.g., 3 ℃ /min) is performed on the material to obtain the T_g, in which the material is under a sinusoidal extensional deformation in the linear range at a fixed frequency (e.g., 1 Hz). The complex dynamic elastic modulus E^* ($E^* = E' + iE''$, E' and E'' are storage modulus and loss modulus, respectively; $\tan\delta = E''/E'$ and δ is the phase angle) is obtained as a function of temperature. The T_g is obtained from the peak temperature of either $\tan\delta$ or E'', the value determined from $\tan\delta$ is generally higher. Since glass transition shows kinetic dependence, the value of T_g varies with the applied frequency, i.e., it increases as frequency increases. In general, the DMA experiments described above are applicable to bulk samples with the sample mass of 100 mg or more.

Recently, the thin film DMA technique with mass requirement of approximately 5 mg has been successfully employed in measuring the T_g of conjugated polymer, in which the thin film is enclosed into a stainless steel pocket,[124] or drop-casted on either a polyimide (PI) substrate[125] or a woven glass fiber[126]. It has been suggested that DMA is more sensitive to the T_g of conjugated polymers compared to the differential scanning calorimetry (DSC). **Figure 3** presents the schematic instrument set-up utilized by Sharma et al., in which the solution of poly[[2,3-bis(3-

octyloxyphenyl)-5,8-quinoxalinediyl]-2,5-thiophenediyl] (TQ1) was drop-coated onto the glass fiber.[126] The measurements were then performed on the TQ1 coated glass fiber. Although, in this case, T_g can also be obtained from the peak of $\tan\delta$ or E'', since the sample geometry is unspecified, it is not able to acquire the absolute modulus value. In addition, as pointed out by Xie and co-workers, besides glass transition, other thermal transitions often observed in conjugated polymers, such as melting and smectic-to-isotropic transition, also lead to peak in $\tan\delta$, which potentially could be challenge to accurately differentiating various phase transitions.[25,127]

In addition to the extensional deformation, the material can also be measured under shear deformation. In this case, the disk-shaped sample is prepared and measured with a rotational rheometer, and the complex dynamic shear modulus G^* ($G^* = G' + iG''$, G' and G'' are storage modulus and loss modulus, respectively; $\tan\delta = G''/G'$ and δ is the phase angle) is obtained. Similarly, the value of T_g can be obtained from the peak temperature of either $\tan\delta$ or G''. This type of measurements have been successfully reported on different polymers.[25,128,129] **Figure 4** displays the dynamic moduli for a variety of poly(3-hexylthiophene) (P3HT) with different regioregularities measured by temperature ramp.[25] The backbone T_g and side chain T_g are readily obtained from the peaks in G'' response.

In addition to obtaining T_g from the temperature sweep measurements, it has been shown by McKenna and coworkers[130–133] that the T_g can also be obtained from the measurement of frequency sweep at different isotherms, in which the data in the frequency space are converted to the temperature space for a certain frequency (e.g., 0.01 rad/s, which corresponds to 100 s relaxation time) when the time-temperature superposition principle[30] holds. The mass requirement for dynamic rheometry can be as low as ~15 mg,[25,132] much less in comparison to bulk DMA measurements, but still larger than thin film DMA technique mentioned above.

Furthermore, since it measures the absolute value of moduli and viscosity, it is able to identify different thermal transitions, which overcomes the shortcomings in thin film DMA. However, since the rheometry measures the bulk properties, it is still questionable to apply the information extracted from rheometry to thin films.

In addition to BDS, DMA and advanced rheometry, other technique like Neutron Backscattering Spectroscopy[134,135] were used to study the dynamics of the polymer, which is indirect way to probe T_g.

3.3 Thermodynamic measurements

3.3.1 Volume dilatometry

Dilatometry is a technique to measure the dimensional change (expansion or shrinkage) of a material as a function of time, temperature, pressure etc.,[35] from which the T_g can be obtained. A volume dilatometer is used to investigate the pressure-volume-temperature (PVT) response. A typical response of the specific volume for an amorphous material over a certain temperature range under isobaric condition is depicted in Figure 2. At the glass transition region, a change in the slope of the specific volume versus temperature is observed, and T_g is readily determined from the intersection of the liquid line and glassy line. Although this technique has long been utilized to investigate the T_g and physical aging of traditional polymers, its application in conjugated polymers is limited due to the relatively large sample mass requirement (~ 1 g).[123]

3.3.2 Differential scanning calorimetry

Differential scanning calorimetry (DSC) is a thermal analytical technique that has been widely used to measure T_g of the polymers in different size scales. It measures the heat flow rate difference

between the sample and reference as a function of temperature and time, and subsequently measures the heat capacity (C_p) of the sample.[136]

In general, for a T_g measurement, it consists of two heating scans and one cooling scan. In the first heating scan, the sample is heated to high temperature (above T_g) to remove its thermal history, for example the physical aging for amorphous polymer. (For the semicrystalline polymers, the sample needs to be heated above the melting temperature T_m to melt the existing crystalline content) Then it is cooled down to low temperature (below T_g) at a certain cooling rate (e.g., 10 °C /min). After that, it is reheated to high temperature at the same rate and the T_g is the determined from the second heating scan, in which a step change in C_p (ΔC_p) or heat flow is observed in the glass transition regime, as shown in Figure 5. We note here that, historically because of instrumental limitations, it is a common practice to measure the T_g from the heating scan, despite that the T_g can only be correctly determined from the cooling experiments.[137–139] In fact, the heating scan measures the fictive temperature T_f, which was introduced by Tool[140] to study the state of inorganic glass in the glassy state, and can be calculated by Moynihan method.[28] In the case of unaged sample, in which the sample is cooled into the glassy state followed by an immediate heating at same rate, the heating scan yields the limiting fictive temperature T_f', which is equivalent to T_g measured on cooling.[27,137–139]

Depending on the size scale of the polymers (e.g. film thickness), different types of DSC can be used. The conventional DSC (standard DSC and modulated DSC), which has the maximum cooling rate of up to hundreds several tens K/min, normally measures applies to the bulk sample with the mass of several milligram. It also has the capability to measure the polymer ultrathin film in the nanometer scale. However, the sample preparation is time consuming since it requires the stacking of several hundred layers of ultrathin film in order to meet the mass requirement.[32,86,141–

145] With the new developments of the nanocalorimetry,[87,146–154] including flash DSC and AC-chip calorimetry (We note here that the modulated DSC and the AC-chip calorimetry are considered as dynamic measurements of T_g),[18,155,156] which has the mass requirement of nanogram, measuring the T_g of sub-100nm a single layer of polymer ultrathin film with DSC becomes possible and has drawn increasing attention.[29,155–177]

The application of DSC in characterizing T_g for conjugated polymers has been elusive. For the illustration purpose, **Figure 5** presents the DSC traces during second heating scan for oligofluorenes and polyfluorene.[122] A step change in heat flow associated with glass transition is observed in all the DSC traces for oligofluorenes. The value of T_g increases from 253 K for the dimer to 316 K for heptamer with the heat capacity change ΔC_p approximately of 0.25~ 0.3 J/g·K for all oligofluorenes.[122] However, in the case of the polyfluorene, T_g is not detectable, which has been attributed to the increased heat of fusion in the endothermic peak at high temperature as a consequence of mesophase organization[122] on cooling which leads to less amorphous fraction.

Conjugated polymers typically show a small change in heat capacity ΔC_p near glass transition, causing difficulties in characterizing T_g. Here, the T_g we referred to is the backbone T_g, and the side-chain T_g, located at a low temperature can often be detected by DSC. There are several factors that may possibly contribute to the observation of the difficulty in characterizing T_g for conjugated polymers because of the small change in heat capacity ΔC_p. (Here, the T_g we referred to is the backbone T_g at high temperature, since the side-chain T_g at low temperature can often be detected by DSC.) First, the backbone of conjugated polymer has high rigidity. By adding the side-chain, although it reduces the crystallinity and subsequently increases the solubility, it introduces steric constraints, and the backbone concentration is diluted, which then results in a low ΔC_p at the glass transition.[178,179] In the case of traditional coil polymers, for example, poly(n-alkyl methacrylates),

Donth reported ΔC_p decreases from approximately 0.3 J/g·K to 0.1 J/g·K as the number of carbon in the alkyl increasing from 1 to 6.[180] Another example is the second-generation dendronized polymer, in which the discrete dendronized side groups are grafted on the backbone and resulting a stiffened backbone the molecule taking the extended cylindrical configuration, a low ΔC_p of 0.076 J/g·K was reported by Qian et al.[132] Second, many conjugated polymers are semicrystalline, since the crystalline content does not contribute to the heat capacity change during the glass transition, ΔC_p is further reduced due to the decrease of amorphous fraction.[179,181] In addition, it has been commented that the regular semicrystalline polymers often exhibit a broad glass transition, which leads to the difficulty of T_g determination.[182] We believe this is also true for the conjugated polymers, for example, the diketopyrrolopyrrole (DPP) based polymers whose T_g cannot be readily obtained from DSC.[183–185] Third, indeed ideally the first heating scan removes should remove the thermal history, i.e., melts the crystalline fraction, if many conjugated polymers could still crystalize under the cooling rate of accessible by standard DSC, the crystallization may still take place on cooling. This issue could be resolved using a fast scanning DSC, which has the cooling rate in the order of 10^6 K/s. Another difficulty for removing crystalline domain in conjugated polymers is their high melting point. In many cases, the melting temperature (T_m) is close to or even higher than the degradation temperature (T_d). In the case of AC-chip calorimetry, which is a type of dynamic measurement and has high sensitivity of ~ 50 pJ/K,[156] it is able to detect the T_g of conjugated polymers, such as poly(2,5-bis(2-decyltetradecyl)-3,6-di(thiophen-2-yl)diketopyrrolo[3,4-c]pyrrole-1,4-dione-alt-thienovinylthiophene) (DPP-TVT),[165] whose T_g cannot be detected by the standard DSC.[186] One challenge is that the AC-Chip calorimetry cannot be readily accessed. Modulated DSC has been utilized to characterize the T_g for poly(3-

alkylthiophenes)[129] and Phenyl-C61-butyric acid methyl ester (PCBM)/conjugated polymer blends,[187,188] however, its sensitivity is not comparable to AC-chip calorimetry.

3.4 Pseudo-thermodynamic measurements

3.4.1 Ellipsometry

Based on the work of Beaucage et al.,[189] Keddie et al.[75,88] first investigated the thickness dependence of T_g for polymer thin films using ellipsometry, which is one type of the dilatometric measurements.[15,179] It characterizes the thickness and refractive index of a thin film by measuring the polarization change of light reflected off of the thin film. Unlike the volumetric dilatometry, ellipsometry only measures the change in one dimension, i.e., thickness, and relates it to the thermal expansion of the material.[34] In the T_g measurement, the ellipsometric angle which is linear proportional to the thickness and refractive index[75] is measured as a function of temperature, and the T_g is determined from the discontinuity in ellipsometric angle, thickness, or refractive index. Besides ellipsometry, other related dilatometric measurements of thin film thickness and subsequently T_g include X-ray reflectivity[190,191] and neutron reflectivity[192,193].

The application of ellipsometry in characterizing the T_g of conjugated polymers has been successfully demonstrated by different groups[194–202] for various conjugated polymers. **Figure 6** plots the temperature dependence of ellipsometric angle Ψ for the supported poly[N-9'-heptadecanyl-2,7-carbazole-alt-5,5-(4',7'-di-2-thienyl-2',1',3'-benzothiadiazole)] (PCDTBT) ultrathin film with different thicknesses, measured by Wang et al. [197] as an example. The T_g is determined from the intersection of two linear fits. A decrease in T_g with film thickness is observed. Although ellipsometry can be used to measure the T_g of conjugated polymer thin film, to the best of our knowledge, only the materials with T_g above room temperature have been investigated.

3.4.2 Brillouin light scattering

Brillouin light scattering can be used to measure the T_g for polymers both in bulk and thin film. For the bulk measurement, the temperature dependence of the bulk longitudinal phonon frequency is measured; for thin film measurement, it measures the frequency of the second lowest frequency acoustic mode S_0. In both cases, the T_g can be determined from the temperature at which the measured property shows an abrupt slope change.[92] It was utilized to measure the T_g of PS free-standing thin film by Forrest et al., a T_g depression of 70 K for a 29 nm thick film was observed.[92]

3.4.3 Plasmonic nanospectroscopy

Plasmonic nanospectroscopy has recently been utilized to characterize the T_g for polymer thin films.[203] In this technique, a glass slide is decorated with noninteracting gold (or silver) nanodisk sensors, which is then coated with a thin layer dielectric spacer, on which the polymer thin film is deposited. It monitors the shifts ($\Delta\lambda_{peak}$) in the spectral peak of the localized surface plasmon resonance (LSPR) of Au sensors caused by local refractive index changes of thin film, as a function of temperature. Similarly, the discontinuity in $\Delta\lambda_{peak}$ determines the T_g. This validity of this method was first confirmed by examining the T_g of PMMA thin films on silica substrate and an increase in T_g with decreasing of film thickness is observed,[203] which is consistent with the results reported by Keddie et al.[88] using ellipsometry. Later, it also shows great success in terms of measuring the T_g for conjugated polymer thin films.[204,205] **Figure 7** depicts the $\Delta\lambda_{peak}$ as a function of temperature for five different conjugate polymers along with PMMA. It is clearly seen that besides the T_g, this technique is able to detect other thermal transitions including melting and nematic-isotropic transition.

3.4.4 UV-Vis spectroscopy

UV-vis spectroscopy is a widely used material characterization technique. Recently, its application in determining the T_g for conjugated polymer films was demonstrated by Root et al.[206] It is a common observation that for the conjugated polymer films, the order aggregates formed during the thermal annealing lead to the shift in the UV-vis absorption spectrum. Based on this, they proposed that T_g can be estimated from quantifying the difference in the UV-vis absorption spectrum between annealed sample and as-casted sample. They defined a parameter, deviation metric (DM_T), which is the sum of the difference between annealed and as-casted sample. **Figure 8** plots the annealing temperature dependence of UV-vis spectra along with DM_T for poly(3-butylthiophene) (P3BT), and T_g is extracted from the intersection of two linear fits from Root et al.[206] They also tested this method on a variety of semicrystalline conjugated polymers and amorphous conjugated polymer, however, this technique fails to detect the T_g of amorphous conjugated polymers since it relies on the formation of ordered aggregates during thermal annealing. In addition, the validity of this technique on the conjugated polymers with T_g below room temperature is questionable.

3.4.5 other techniques

In addition, there are other pseudo-thermodynamic measurements to measure the T_g, including positron annihilation lifetime spectroscopy (PALS),[90] fluorescence probe intensity[98] and local thermal analysis[89]. Due to limited by the space, we will not discuss them in full detail here.

3.4.6 summary

As we discussed above, there are many techniques that can measure T_g. We attempt to summarize the potential advantages and disadvantages for the experimental techniques with a focus of their complexity, materials requirements, capability to measure ultrathin film, to

determine their potential use in measuring T_g for conjugated polymers. The result is summarized in the **Table 1**.

4 Glass transition for conjugated polymers

Despite various testing methods of T_g for traditional polymers, there is a noteworthy lack of T_g information for conjugated polymers in the literature, which makes it hard to clearly understand the mechanical performance and morphology stability for the application of organic electronic devices.[11,207] This is mainly attributed to the difficulty in obtaining the T_g value by traditional testing methods (e.g. DSC) for donor-acceptor polymers. There are several reasons contributed to this difficulty. First of all, conjugated polymer synthesis generally is performed in small batch and has batch-to-batch variation. Typically, the planar and rigid backbones of conjugated polymers lead to weak backbone relaxation signal that challenge the usage of a normal DSC. Fast scanning DSC or AC-chip calorimetry are required to obtain good signal, especially for donor-acceptor polymers.. Secondly, only limited amount of donor-acceptor polymers can be obtained in a single batch (typically less than 500 mg), while standard rheology or DMA tests typically requires more than 100 mg of material. While there are new developments in both techniques to all measurement done on much less materials (e.g. 30 mg per run[126,127,208]). Also, for organic electronic devices, conjugated polymers were typically processed into thin-film state (< 100 nm thick), at which the T_g of conjugated polymer thin films could deviate from the bulk polymer, thus a clear understanding of the relationship between film thickness and T_g is required for real world application. Up to now, the commonly reported methods for detecting bulk T_g is the DMA test where the sample was made through casting polymer solutions onto a substrate (Kapton film or glass fiber), while thin-film T_g was typically obtained by DSC, fast scanning DSC, AC-chip calorimetry and ellipsometry.

Unlike traditional amorphous polymers, establishing a general model to predict the T_g of conjugated polymers is extremely hard owing to the highly varied building blocks introduced by backbone and side-chain engineering. That being said, when discussing glass transition for a conjugated polymer, it is important to specify their backbone and side chain structure. For polythiophenes family, the T_g can vary over 100 °C (). Therefore, classification of conjugated polymers into different groups with similar chemical moieties is needed for a better understanding various building block's effect on thermomechanical property. Here, we will cover various conjugated polymers including polythiophenes and polyfluorenes, donor-acceptor type of conjugated polymers like IDT-based, isoindigo-based and DPP-based polymers, as well as other less reported conjugated polymers are reviewed and discussed.

4.1 Polythiophenes

The development of polythiophenes (PT) starts from low molecular weight and amorphous polymers synthesized by electrochemical polymerization with a low mobility on the order of 10^{-5} $cm^2/(V{\cdot}s)$.[209] Soon after, in order for solution processing, alkyl side-chain substituted polythiophenes were synthesized.[210,211] Among all of them, highly aggregated semicrystalline regioregular poly(3-hexylthiophene) (P3HT) was independently synthesized by Rieke[212] and McCullough[213] in the early 1990s. Since then, it has been the predominantly reported conjugated polymer in the literatures.

As a model system, the poly(3-alkylthiophene)s are ideal platform to study the influence of the sidechain's influence on the T_g. Unlike π-conjugated backbones determining the optoelectronic properties of the resulting polymers, peripheral flexible solubilizing side chains initially were introduced just to facilitate synthesis as well as processing. The role of side chain has not attracted much attraction until recent years when people start to realize their huge influence on packing

structure of crystalline domain and the thermomechanical performance of conjugated polymers.[214] **Figure 9** depicts the backbone T_g (α-transition) and side-chain T_g (β-transition) of poly(3-alkylthiophene)s (P3AT)s as a function of linear alkyl side chain length. It is readily seen that for unsubstituted polythiophene, it features a T_g of ~120 °C,[215] with increasing linear alkyl side-chain length (0 to 8 carbons), the T_g drops significantly as a result of the plasticization effect from side chains. For example, poly(3-butylthiophene) (P3BT) showed a T_g of 45 °C, followed by 12 °C for P3HT and -13 °C for poly(3-octylthiophene) (P3OT); however, when the side chain is further lengthened, with the occurrence of side chain crystallization, T_g increases,[129] which is similar to poly(n-alkyl methacrylates) and poly(4-alkyl styrenes).[65] The backbone T_g of P3AT depends on the regioregularity, as depicted in **Figure 9**, regioregular P3AT has a higher backbone T_g compared to regiorandom P3AT, due to the higher chain rigidity and the presence of less mobile amorphous domain under the nanoconfinement of the crystalline domain; while the side chain T_g is relatively insensitive to the regioregularity as suggested by Pankaj et al.[216] Beside the side chain length, the structure of the side chain also plays an important role, as listed in **Table 2**, P3OT and poly(3-ethylhexylthiophene) (P3EHT) have same number of carbons in the side chain, however, P3EHT shows a T_g of 24 °C,[217] while P3OT has a T_g of -13 °C.[129]

In addition to the side-chain modification of polythiophenes, the backbone structure was engineered by adding on a centrosymmetric repeat unit, thieno-[3,2-b]thiophene to improve the microstructural ordering, and charge transport property. One example is poly(2,5-bis(3-alkylthiophen-2-yl) thieno-[3,2-b]thiophene) (PBTTT).[218] The extra free volume created by the unsubstituted thieno-[3,2-b]thiophene central ring allows the side chain from an adjacent molecule to interdigitate with each other.[6] This promotes the ordering of packing between PBTTT polymer chains, but in the meantime, the T_g and brittleness were also significantly raised when compared

with P3HT.[219–221] The case of PBTTT indicated the important role of sidechain interdigitations on glass transition.

4.2 Polyfluorenes

As an important class of electroactive and photoactive material, the investigation of polyfluorene polymer was dated back to the early 20th century. In contrast to P3ATs consisting of isolated thiophene rings and linear side chains with significant freedom to sample conformational space, polyfluorenes, on the other hand, contain a rigid biphenyl unit with limited internal rotational entropy.[222] Therefore, in general, polyfluorene has a higher T_g when compared with P3AT having the similar fraction of side chains. For example, as listed in **Table 3**, poly(9,9-dihexylfluorene) (F6), poly(9,9-dioctylfluorene) (F8), and poly(9,9-didodecylfluorene) (F12) have T_gs of approximately 94 °C, 72 °C and 47 °C, respectively;[223] while P3OT, P3DT and P3DDT show much lower T_gs of approximately -13 °C, -25 °C and -18 °C, respectively.[129]

Similarly, the T_g of polyfluorenes can be tuned by the backbone engineering through copolymerizing PFO with a second building block. Poly(9,9-dioctylfluorene-co-bithiophene) (F82T), which essentially consists of the F8 backbone and two additional thiophene units, features a relatively high T_g of approximately 73~109 °C as a consequence of the reduction in the side chain fraction.[224–226] By introducing even bulkier building blocks to the backbone structure, the side chain content is further reduced meanwhile the chain rigidity is increased, which consequently raises the T_g. For example, as listed in **Table 3**, inclusion of a rigid fused ring benzothiadiazole (BT) unit to F8 backbone results in a much higher T_g of ~ 135 °C for poly(9,9-dioctylfluorene-co-benzothiadiazole) (F8BT);[227] and poly(2,7-(9,9-dioctyl-fluorene)-alt-5,5- (4′,7′-di-2-thienyl-2′,1′,3′-benzothiadiazole)) (APFO-3 or PFTBT) features a lower T_g of approximately 130 °C[228–230] compared with the T_g of poly(2,7-(9,9-dioctyl-fluorene)-alt-5,5- (4′,7′-di-2-thienyl-2′,1′,3′-

diphenyl-quinoxaline)) (APFO-18) and poly(2,7-(9,9-dioctyl-fluorene)-alt-5,5(2,3,6,7-tetraphenyl-9,10-dithien-2-yl pyrazino[2,3-g] quinoxaline)) (APFO-Green9), which are around 142 °C[231] and 177~192 °C,[200,231] respectively, because of the bulkier building blocks in the latter two cases.

Besides adding building blocks to the linear polymer backbone, kinked polymer backbone is another alternative backbone engineering method. In this case, the rotational entropy is reduced, resulting in a higher T_g. For example, poly(9,9-dioctylfluorene-co-N-(4-butylphenyl)diphenylamine) (TFB) with a kinked polymer backbone has a high T_g of ~ 156 °C.[201] Upon branching the side chain on the triphenylamine unit, a TFB derivative features a lower T_g of ~ 140 °C.[232]

4.3 Donor-acceptor conjugated polymers

Based on the early investigation of polythiophenes and polyfluorenes, donor-acceptor conjugated polymers (D-A CPs) were developed to obtain a controlled HOMO/LUMO energy level, lower bandgap, as well as reduced conformational energetic disorder.[6,236,237] This design approach achieved superior charge carrier mobility in many D-A CPs due to a coplanar backbone conformation which minimizes the backbone torsion and steric hindrance between the donor and acceptor conjugated units, leading to large overlap in the delocalized electronic cloud. Nevertheless, the rigid nature of these building blocks makes D-A CPs even less soluble, and the most widely applied strategy to improve the solubility is introducing long and branched sidechains. Moreover, bulkier moieties such as branched alkyl side chains can result in a more twisted and less rigid backbone under the influence of the steric hinderance, thus reduce the tendency for form ordered aggregates or crystallization.[238,239] Clearly, there are many unsolved questions, including T_g, in the study of D-A CPs with the large variety of combinations of building blocks, here we will

only cover several commonly used D-A CPs including indacenodithiophene-based (IDT), diketopyrrolopyrrole-based (DPP) polymers.

4.3.1 Bridged and fused family

With high content of branched alkyl side chains (almost 70% of mass content), as listed in **Table 4**, all three IDT[240] polymers possess a T_g below room temperature, despite their rigid backbone structure. This is attributed to the long and branched alkyl side chain increasing the degree of freedom and the configurational entropy of the polymer chain. Additionally, these polymers exhibit weak intermolecular interactions and low degree of crystallinity from X-ray diffraction (XRD) measurements.[241] The charge transport mobilities (μ) of these polymers remain relatively high (0.06~0.20 $cm^2\ V^{-1}\ s^{-1}$) and increase with backbone planarity.[241]

At a lower fraction of alkyl side-chain, PTB7, PTB7-Th, PCDTBT feature a much higher T_g of ~ 130 °C, although they seem to have less rigid backbones compared with IDT-based polymers.[197,242,243] To improve the thermal stability of the solar cell, Kesters et al. synthesized a series of side-chain functionalized poly (2, 6- (4, 4-bis (2-ethylhexyl) -4H-cyclopenta (2, 1-b; 3, 4-b′)-dithiophene) -alt-4, 7- (2, 1, 3-benzothiadiazole)) (PCPDTBT) having high T_g of ~ 174, 198, and 161 °C,[244] as listed in **Table 4**, which is presumably related to the rigid backbone structure and low side chain content. Also included in **Table 4** are a series of dithienosilole/thienopyrrolodione copolymers (PDTSTPDs) with similar side chain content, their T_gs are comparable.

4.3.2 Diketopyrrolopyrrole (DPP) and Isoindigo family

Among various D-A CPs containing bridged and fused ring structure, the high-profile DPP-based and isoindigo-based polymers[246] are drawing more and more attentions lately. Typically,

the synthesis of DPP polymers is through palladium-catalyzed Suzuki, Stille and Buchwald-Hartwig polycondensation, or electropolymerization.[6] DPP polymers have relatively ordered lamellar structure and strong packing behavior, as evidenced by their higher order of lamellar peaks (like (200) and (300) peak) and clear (010) π-π stacking peak shown in XRD.[247] Owing to the close intermolecular packing distance and nearly torsion-free backbone, which arise from the dipolar fused lactam carbonyl units and planarity of the thiophene flanking units, the DPP polymers show exceptional charge transport mobilities.[6,248] However, due to the strong intermolecular interactions, long and branched alkyl side chains on both nitrogen pyrrole groups are commonly attached in order to improve the solubility.[249,250] Therefore, DPP polymers usually have a high content of side chains as listed in **Table 5**, and the T_g of DPP polymers is close to the room temperature as well.

Besides side-chain length, the structure of the side chain also has a strong influence on the backbone T_g of DPP polymers. Compared with linear side chains, branched alkyl side chains could significantly alter the T_g. As presented in **Table 5**, the T_g drops from 4.3 °C for P1(C16-PTDPPTFT4) to approximately -48 °C for both P2(C8C10-PTDPPTFT4) and P3(C8C10-PT2DPPT2FT4) after introducing a longer and branched side-chain, according to the report. The -48 °C could be the sidechain T_g and further experiment is needed to clarify. This could result from the depressed crystallization of alkyl side-chain and higher conformational entropy created by more chain ends.[208] Moreover, the branch point position is expected to affect the backbone T_g depending on the introduced steric hinderance, which is a topic that has not been widely investigated yet.

The nature of chemical moiety in the backbone is influential on backbone T_g. Driven by the need of low band-gap and wide-range absorption spectrum, much efforts have been devoted to

copolymerization of the dithienyl-DPP core and a wide range of donor units including bi-[251] ter-[249] and quater-thiophene, thienothiophene,[250] thiazolothiazole,[252] dithienopyrrole,[253] phenyl,[254] and benzothiadiazole (BT).[255] The addition of isolated thiophene units or fused thiophene rings leads to a reduction in the side chain fraction, and thus increase in the T_g of DPP polymers. With different numbers of isolated thiophene units in the backbone, the T_g increased from -4.0 °C for P(DPPT) to 12.0 °C and 19.0 °C for P(DPPT2) and P(DPPT3), respectively. Similarly, the T_g measured with thin film DMA goes up from -4.0 °C for P(DPPT) to 2.8 °C and 4.1 °C for P(DPPTT) and P(DPPTTT) with fused thiophene rings, respectively, (**Table 5**). However, AC-chip calorimetry for P(DPPTTT) gives a T_g of 22 °C, much higher than that from DMA, which is consistent with the conformational freedom of the structure.[256] This suggests that extra caution needs to be paid when interpret the results from DMA.[127] Following this trend, the T_g of conjugated polymers can be engineered by controlling the side-chain fraction. Through the addition of extra side chains to the thiophene unit in P(DPP3T), the weight fraction of the side chain was increased to 62.5%. Consequently, the T_g of this new polymer P(DPP3T-C8) dropped from 19.0 °C to -11.8 °C. The T_g of P(DPPTT)-C8C10 measured with AC-chip calorimetry shows a T_g reduction as the size decreases from bulk to nanofiber, owing to the confinement effect.[10] This is similar to the observations in the regular polymers.

The application of isoindigo on the organic semiconductor was first discovered by Mei et al. in 2010.[257] Similar to the DPP polymers, the backbone T_g of isoindigo-based polymers cannot be readily observed from DSC curve.[258–260] Recently, Schroeder et al. characterized the T_g of isoindigo-bithiophene copolymer with 2-octyldodecyl side chains measured with different experimental techniques, including standard DSC, AC-chip calorimetry, and thin film DMA where the material was drop-casted on Kapton film.[125] A backbone T_g of 43 °C was observed from thin

film DMA. For the side chain T_g of -27 °C from DMA shows a good agreement with the value obtained from standard DSC, i.e., -37 °C, however, the AC-chip calorimetry gave much lower side chain T_g of -82 °C. The authors did not comment on the possible origins of such great discrepancy.

4.4 Other conjugated polymers

Poly(p-phenylenevinylene) (PPV) is a well-known conjugated polymer for being applied to the first polymer-based light emitting diode (LED) in 1990.[263] Because of its stability, processability, and electrical properties, a large number of PPV derivatives have been synthesized for LED and organic solar cell applications. Almost invariably, the T_g of side-chain substituted PPVs greatly deviates from the unsubstituted PPV. The two most common derivatives poly (2-methoxy-5-(2′-ethyl-hexyloxy)-1, 4-phenylenevinylene) (MEH-PPV) (T_g ~ 65~66 °C.[264–266]) and poly [2 - methoxy-5- (3′, 7′-dimethyloctyloxy) -1, 4-phenylenevinylene] (MDMO - PPV) (T_g ~ 18~50 °C.[188,265]) feature a significantly lower T_g than the unsubstituted PPV (T_g~ 220 °C.[267]) due to their ethyl-hexyloxy and a longer dimethyloctyloxy side-chain, respectively. It is also seen that the addition of a bulky pendant group onto the end of a flexible alkyl side-chain can reduce the segmental mobility. This is shown in poly (2-methoxy-5-(2′-phenylethoxy)-1, 4 phenylenevinylene) (MPE-PPV), which features a high T_g of ~ 111 °C with a phenyl-ethyloxy side chain (**Table 6**).[188,268]

For TQ series of polymers consisting of alternating thiophene and quinoxaline monomers, the influence of backbone irregularity on T_g has been observed. As presented in **Table 6**, TQ1 and TQ-8A exhibit fairly high T_g of ~100 °C.[126,269] Surprisingly, a slight increase in the torsion angle results in a significant decrease in T_g (~50 °C) for TQ-F. As for TQ-N, the incorporation of the

pyridopyrazine unit leads to a more asymmetric polymer backbone and thus a lower T_g (~50 °C).[269]

Recently, several reports have described the improvement of stretchability of polymer semiconductors by incorporating non-conjugated spacers. Interestingly, it is observed that long and flexible conjugation breakers in the backbone can improve the ductility and lower elastic modulus without significantly affecting the charge mobility.[125,270,271] Meanwhile, as suggested by molecular dynamics simulation, the dynamics of polymer chains can be enhanced by the non-conjugated flexible linkers.[270] On the contrary, with the insertion of a conjugated spacer like thiophene unit into the polymer backbone while maintaining the same side chain length, PA4T-BC2-C10C12 shows a 25 °C increase in T_g than that of PA3T-BC2-C10C12 (chemical structures shown in **Table 6**).

5 Empirical design rule for tuning T_g for conjugated polymers

In section 4, we delineated reported T_g for conjugated polymers. Although the T_g of conjugated polymers is not clearly understood, several empirical structure-property relationships developed from the classical polymer physics theory such as the influence of molecular weight, chain rigidity, side-chain architecture on T_g, can still be utilized to rationalize the thermal behavior of conjugated polymers.[207] In particular, conjugated polymers are highly heterogenous in their chemical structures, that is to say, the backbone of the polymer is composed of rigid conjugation building blocks while the side-chain is mostly flexible. Thus, to correlate the T_g of a conjugated polymer with its chemical structure, it is vital to elucidate the nature and extent of influence from individual chemical motif, where the flexibility of the main chain and the weight fraction of the side chain should be considered to be the principal parameters.[272]

5.1 Role of side chains: not just a knob for tuning solubility

Tracing back to the reported work on the non-conjugated polymers like poly(n-alkyl acrylate)s and poly(n-alkyl methacrylate)s, the T_g is strongly affected by side-chain length. In **Figure 10a**, we present a schematic representation of the effect of n-alkyl length on the T_g as an illustrative example.[272] A decrease in T_g with the increase of n-alkyl length is observed until the number of methylene groups in side chain (n) reaches a critical number n_c. The value of n_c varies with polymer structure, for instance, poly(n-alkyl acrylate)s has a n_c of 9 whereas the n_c of poly(n-alkyl methacrylate)s is 12.[272] As n further increases, the side chain crystallization takes place, which reduces the main chain mobility and the corresponding T_g starts increasing.[65,272] This effect is echoed the in the previous section 4.1 when discussing the sidechain length for P3HT. One thing worth noting is that the role of side-chain structure is another very important factor, which needs to be further demonstrated in the future work. For example, conjugated polymers, especially the donor-acceptor type polymer, there are mainly two types of side chains being used: linear and branched alkyl side chains. For branched chain, the branched point is another point worth discussing.

Furthermore, we compiled a library of conjugated polymers reported and plotted their backbone T_g vs weight fraction of side-chains, as shown in Figure 10b, in hope to discover if there is a relationship exist. To keep the plot simple, we did not differentiate rigidity of the backbone building block and as well as sidechain type and branch position. **Figure 10b** presented a clear trend where the T_g decreases with the content of the side chain. Similar to low molecular weight diluents, side-chain acts like a plasticizer, which increases the free volume of the polymer system and subsequently lowers the T_g. The major difference between side-chain and plasticizer is that side chains are attached directly to the backbone, so that this strong interaction allows the

plasticization effect to disperse more evenly along the main chain. Besides, polar side chains, such as alcohol-functionalized side chain, exhibit strong interaction force, therefore it may exhibit anti-plasticization effect to the conjugated backbone. Hence, the side chain engineering is a powerful tool to tune the T_g of conjugated polymers.

5.2 Role of Backbone: The route not being heavily studied

In addition to the influence of side chains, the backbone chemical moiety also has a significant impact on the backbone T_g of conjugated polymers through affecting the backbone flexibility. Although the backbone structure of D-A polymers is getting complicated with more and more bridged and fused rings, still they can be treated as copolymers of various complex moieties. Several approaches have been proposed for the estimation of T_g with the knowledge of thermal properties of individual pristine components, based on the additivity of basic thermophysical properties. One of the most well-known equation for predicting the T_g of amorphous mixtures and random copolymers is so-called Fox equation:[273]

$$\frac{1}{T_{g,mix}} = \sum_i \frac{\omega_i}{T_{g,i}} \tag{11}$$

Here, $T_{g,mix}$ and $T_{g,i}$ are the glass transition temperature of the mixture and the components, respectively. ω_i is the weight fraction of the component i. In general, the Fox equation has relatively good predictability and accuracy for the T_g of (miscible) polymer blends and statistical copolymers.

As for semiconducting D-A conjugated polymers, which can be treated as copolymers of the donor unit and the acceptor unit, the Fox equation can only be applied for a rough prediction of T_g. For example, P(DPPT) and non-substituted polythiophene exhibit a T_g of -4.0 °C and 120 °C, respectively. Based on Fox equation, P(DPPT2) consisting of a DPPT unit and a thiophene unit will have a T_g of 3 °C while the detected T_g is 12 °C. Similarly, the measured T_g is 19 °C for P(DPPT3), and the predicted value is and 13 °C. Although the predicted T_g is different from experimental results, but the trend of increasing T_g with more pendent groups in the backbone stays valid. Along this line, as long as the T_g of individual components that

constitutes the conjugated polymer is known, the T_g of the whole conjugated polymer can be predicted with reasonably good accuracy using Fox equation even before synthesis.

6 Future look

In this review, we have introduced the glass transition phenomena and summarized previous works related to conjugated polymers. We discussed several empirical design rules can be inherited from the classical polymer system to conjugated polymers. A holistic picture of glass transition phenomena for conjugated polymer is still not clear yet. With the recent surge of interest to design wearable electronics, the glass transition phenomenon is getting increasingly important since a thorough understanding the fundamental design rule would benefit the field tremendously and fuel the next wave of the flexible electronic revolution, such as foldable electronics, stretchable electronics, wearable electronics, and implantable bioelectronics. Here are three questions that we believe are important for glass transition phenomena for conjugated polymers.

6.1 Can one predict, control, make conjugated polymers with arbitrary T_g?

The ultimate goal of studying the T_g of conjugated polymers is to achieve a design rule that can predict, control, make conjugated polymers with arbitrary T_g that suit the end the devices end application. This would require synergistic effort from polymer chemist, polymer physicist, and computation scientist. Systematic tuning the building blocks of the conjugated polymers allows one to pin down respective function groups' effect on glass transition. Combined with the thin film characterization technique for T_g (Fast Scanning DSC, ellipsometry and UV-Vis), the study could also shed new light, especially for donor-acceptor polymers. Specifically, we would direct the reader's attention to the follow questions, which are unique to conjugated polymer's stricture.

1. How does sidechain architecture and chemical composition affect the glass transition phenomena?

Unique to conjugated polymers are their long alky sidechain. The **Figure 10b** in chapter 5 provides a simplified correlation between the T_g with the sidechain chain content. This simplified model did not consider the effect of branch point, chain architecture as well as chain chirality. For example, side chain branch position could greatly affect the melting point of the polythiophenes. P3EHT showed a melting point of approximately 80 ^{0}C,[217,274] much lower than that of P3OT (190 ^{0}C[275]). A related work by Gomez group also pointed to a similar direction, showing that the dynamics of the sidechain at different distance to the polymer backbone is vastly different.[135] The longer distance from the thiophenes backbone, the sidechains has higher mobility. More exotic sidechains (e.g. polyethylene oxides, polystyrene, polydimethylsiloxane) are also worth study. For a detailed review of the side chains used in conjugated polymer, the reader should refer to Ref [221,276]. Polydimethylsiloxane sidechains may provide an unconventional approach to increase the free volume, thus dramatically lower conjugated polymer T_g.

2. What is the role of the backbone structure on the glass transition?

The beauty of conjugated polymers is their versatile tunability in chemical structure. Various chemical functionality can be engineered into the conjugated polymer backbone to fine tune their HOMO-LUMO level. This flexibility in conjugated polymer also means that there would not be a simple to describe the T_g for a given polymer family by one T_g. For a given polymer family, one needs to provide T_g with respective to their specific building structure. Currently, there is a lack of knowledge for the glass transition temperate for individual building blocks such as IDT, Isoindigo, DPP or benzothiadiazole moiety. Obtaining T_g for individual building blocks would provide potential new route to model the T_g from various conjugated polymers.

3. What is the T_g for several emerging multifunctional conjugated polymers as well as conjugated polymers with unconventional architecture?

Another significant difference between conjugated polymer with non-conjugated polymers are the additional interactions involved in their condensed phase. Those potential weak interactions include: π-π interactions, hydrogen bonds, metal ligand coordination bonds. Many weak interaction bonds were successfully designed into conjugated polymer to endow self-healing ability[9,277–279] into conjugated polymers. Previous work by Bao group are great example for demonstrating this capability. The effect of the non-covalent bond on the glass transition is not fully understand and worth further exploration. Block copolymer is another common strategy to endow multifunction into the conjugated polymers.[280–282] There are several recent interests to create biodegradable[283,284] or deformable electronic. Block copolymer could provide the additional block to incorporate new function into the conjugated polymer backbone.

4. What are the new theories to predict the glass transition of the conjugated polymers?

Apart from utilizing the experimental techniques, extensive efforts have been made to investigate the glass transition phenomena in polymers, both in bulk and under confinement, with simulation and theory. For example, the analytical generalized entropy theory (GET) developed by Freed and co-workers has shown great success in describing the glass formation of polymer melts as functions of molecular parameters, including monomer structure, cohesive interaction strength, chain rigidity, plasticization, etc.[63,285–295] In addition, Schweizer and co-workers has been successfully developed and applied the elastically collective nonlinear Langevin equation (ECNLE) to investigate the dynamic for different polymeric systems including polymer melts and thin films.[296–301] Moreover, for polymer thin films, a faster relaxation process near free surface has been reported by simulations.[21,78,302–305]

Recently, there are increasing interest of utilizing the simulations to study the conjugated polymers,[243,306–313] with the focus on the morphology, charge-transport property and solubility, etc. However, the study of the T_g for conjugated polymers is limited.[243,313,314] Lipomi and co-workers investigated the thermomechanical property of P3HT as well as three donor-acceptor polymers (PDTSTPD, PTB7 and TQ1) with molecular dynamic simulations, where the predicted properties including density, modulus, and T_g exhibit good agreement with experimental results.[243,314] Therefore, there is a need to expand our current toolbox by utilizing the simulations to completely understand the structure-property relationship for the conjugated polymers.

6.2 How does physical aging affect conjugated polymers?

One missing ingredient in the investigation of the glass transition of conjugated polymers is the so-called physical aging[315–317] (or structural recovery) phenomenon, which is observed in glass-forming materials at the temperature below T_g. As shown in **Figure 2**, in the glassy state, the material remains nonequilibrium, despites the low molecular mobility, it tends to relax towards the equilibrium due to the excess volume, enthalpy etc. in comparison to the equilibrium state.[318] Hence, the mechanical, electrical and optical properties spontaneously evolve with time. For example, the modulus and yield stress increase with aging time, and material exhibits embrittlement,[319,320] which then affect the long-term performance of the material.

In the early work on the inorganic glass by Tool,[140] it is suggested that the state of a glass is relatively understood if the aging temperature T_a and the fictive temperature T_f, the hypothetic temperature at which the structure of glass is at equilibrium (as illustrated in **Figure 2**), are known. Another measure of the structure of glass is the departure from equilibrium $\delta = (V - V_\infty)/V_\infty$ with V and V_∞ are the instantaneous specific volume and equilibrium volume, as suggested by

Kovacs.[321] It is worth pointing out here that T_f and δ are interchangeable and both can be used to monitor physical aging.[16]

The physical aging for non-conjugated polymers has been deeply investigated by different experimental techniques, including volume dilatometry,[31,321] DSC,[322] dielectric spectroscopy,[323] rheometry,[324,325] etc. Several reviews[16,17,71,318–320,326,327] have been published and the interested readers can refer to those works for details. Importantly, there are several signatures for physical aging of glassy polymers. For example, the aged polymer exhibits a overshoot in enthalpy or volume; In addition, Kovacs[321] catalogued three aging signatures for glassy polymers, intrinsic isotherms, asymmetry of approach and memory effect, which demonstrate the kinetics of structure recovery of polymers being nonexponential, nonlinear and path dependent.[168] The aging rate depends on the aging temperature T_a and the distance from T_g, or in other words, the driving force and the molecular mobility.[32,167] At high T_a, the mobility is high, but the driving force is low; while at low T_a, it is opposite. Hence, it results in a maximum in aging rate as T_a decreases[31] and this is also valid in polymer ultrathin films.[32,328]

The investigations of physical aging in polymer thin films were initially focused on polymer membranes, in which an accelerated aging is observed, and the gas permeability reduces with aging time due to the decrease of free volume.[329–334] Recently, the effect of nanoconfinement, e.g. ultrathin film on the physical aging has drawn significant interest.[32,157,159,162,167,168,326,328,335–343] In comparison to the bulk, despite the lower aging rate, an acceleration in physical aging in terms of the timescale to reach equilibrium is observed at same aging temperature,[32,336] which is related to the depression in T_g. By shifting the aging temperature to the same distance from relevant T_g, Koh and Simon[32] showed that the aging rates for bulk and ultrathin film PS are comparable.

Hence, physical aging is essential for the long-term performance of polymer-based devices. To the best of our knowledge, the study of physical aging for conjugated polymers is limited,[68,244,344–346] which could be a subject worth exploring systematically in the future to get better understanding of the aging effect on the mechanical, optical and electronic property of conjugated polymer thin film.

6.3 How does glass transition affect the charge transport property?

One of the unique properties of the conjugated polymer is their ability to transport charge carriers. The mechanism for the charge transport in conjugated polymer has been heavily studied.[347–350] A general picture is that charges would travel through a heterogeneous microstructure consisting of ordered microdomains surrounded by disordered amorphous polymers. The charge transport is most efficient along the polymer backbone. And they need to hop many times between different chains to cover the channel width. Several design rules were outlined. Notable, 1) improving interchain charge transport though improving limiting step for intermolecular coupling; 2) to endow more robust group into conjugated polymer to enhance the structural resilience to disorder, 3) promote interchain transport by reducing torsion between molecular plant and increasing molecular weight.

One interesting question is the role of chain dynamic in the charge transport process. How does the chain dynamic affect the charge transport property? Instead of using a static picture to describe the transport of charges, what happened to the conjugated polymer above (high local chain dynamics) and below glass transition (in vitrified state) would be allow one to study the effect of the dynamic disorder on the charge transport. Interesting, several high mobility conjugated polymers show glass transition near or below the room temperature, such as some DPP, isoindigo and IDT polymers[241,351] (see the tables above). It is worthwhile explore the difference

for the charge transport at the glassy state, at the viscoelastic state, in liquid crystalline state and in melt state. There are studies reporting the temperature dependent optical and charge transport property.[352–355] The mobility of the conjugated polymer typically increases with increasing temperature due to high activation energy, but eventually drops due to unstable morphologies and disrupted molecular packing.[356] It should be noted that when performing such work, one need to decouple two intertangled effects: 1) influence from activation energy of what?.. 2) changes originated from chain dynamics. Additional, as we descried at the beginning of the review, the dynamic for conjugated is highly heterogenous. Separation the dynamic contribution from the backbone with that of the sidechains could be a challenge. Most characterization technique can determine chain dynamics as a whole. Linking the dynamics of the conjugated backbone with charge transport property can be highly valuable and meantime very challenging. One very unique method that can directly probe the backbone dynamic is to use neutron spectroscopy with selective deuteration labeling. Such method would provide direct evidence how backbone dynamic can influence the charge transport property.

To sum up, standing on the shoulder of giant, the research on the glass transition for conjugated polymers could see tremendous improvement in coming years. A better understanding this parameter would provide valuable knowledges when designing the next generation flexible and deformable electronics.

Acknowledgements

Z.Q. and Z.C. contributed equally to this work. This work is supported by the U.S. Department of Energy, Office of Science, Office of Basic Energy Science under award number of SC0019361 for Z.Q., Z.C. and X.G.. S.Z., X.G. also acknowledge NSF for partial supported through office of integrative activities (OIA) by NSF OIA-1757220. L.G. thanks NSF NRT for provide support. J.X. acknowledges the Center for Nanoscale Materials, a U.S. Department of Energy Office of Science User Facility, and supported by the U.S. Department of Energy, Office of Science, under Contract No. DE-AC02-06CH11357.

Received: ((will be filled in by the editorial staff))
Revised: ((will be filled in by the editorial staff))
Published online: ((will be filled in by the editorial staff))

References

[1] L. Meng, Y. Zhang, X. Wan, C. Li, X. Zhang, Y. Wang, X. Ke, Z. Xiao, L. Ding, R. Xia, H.-L. Yip, Y. Cao, Y. Chen, *Science.* **2018**, *361*, 1094.

[2] H. Chen, Y. Guo, G. Yu, Y. Zhao, J. Zhang, D. Gao, H. Liu, Y. Liu, *Adv. Mater.* **2012**, *24*, 4618.

[3] H.-R. Tseng, H. Phan, C. Luo, M. Wang, L.A. Perez, S.N. Patel, L. Ying, E.J. Kramer, T.-Q. Nguyen, G.C. Bazan, A.J. Heeger, *Adv. Mater.* **2014**, *26*, 2993.

[4] G. Kim, S.-J. Kang, G.K. Dutta, Y.-K. Han, T.J. Shin, Y.-Y. Noh, C. Yang, *J. Am. Chem. Soc.* **2014**, *136*, 9477.

[5] Y. Yamashita, F. Hinkel, T. Marszalek, W. Zajaczkowski, W. Pisula, M. Baumgarten, H. Matsui, K. Müllen, J. Takeya, *Chem. Mater.* **2016**, *28*, 420.

[6] S. Holliday, J.E. Donaghey, I. McCulloch, *Chem. Mater.* **2014**, *26*, 647.

[7] J. Mei, Y. Diao, A.L. Appleton, L. Fang, Z. Bao, *J. Am. Chem. Soc.* **2013**, *135*, 6724.

[8] A. Chortos, Z. Bao, *Mater. Today*. **2014**, *17*, 321.

[9] J.Y. Oh, S. Rondeau-Gagné, Y.C. Chiu, A. Chortos, F. Lissel, G.J.N. Wang, B.C. Schroeder, T. Kurosawa, J. Lopez, T. Katsumata, J. Xu, C. Zhu, X. Gu, W.G. Bae, Y. Kim, L. Jin, J.W. Chung, J.B.H. Tok, Z. Bao, *Nature*. **2016**, *539*, 411.

[10] J. Xu, S. Wang, G.-J.N. Wang, C. Zhu, S. Luo, L. Jin, X. Gu, S. Chen, V.R. Feig, J.W.F. To, S. Rondeau-Gagné, J. Park, B.C. Schroeder, C. Lu, J.Y. Oh, Y. Wang, Y.-H. Kim, H. Yan, R. Sinclair, D. Zhou, G. Xue, B. Murmann, C. Linder, W. Cai, J.B.-H. Tok, J.W. Chung, Z. Bao, *Science.* **2017**, *355*, 59.

[11] D.J. Lipomi, Z. Bao, *MRS Bull.* **2017**, *42*, 93.

[12] S. Wang, J. Xu, W. Wang, G.J.N. Wang, R. Rastak, F. Molina-Lopez, J.W. Chung, S. Niu, V.R. Feig, J. Lopez, T. Lei, S.K. Kwon, Y. Kim, A.M. Foudeh, A. Ehrlich, A. Gasperini, Y. Yun, B. Murmann, J.B.H. Tok, Z. Bao, *Nature*. **2018**, *555*, 83.

[13] G.B. McKenna, *Glass Formation and Glassy Behavior, in Comprehensive Polymer Science, Vol. 2, Polymer Properties*, Pergamon Press, **1989**.

[14] G.B. McKenna, *Nat. Phys.* **2008**, *4*, 673.

[15] G.B. McKenna, S.L. Simon, *Chapter 2 - The glass transition: its measurement and underlying physics*, in: S. Z. D. Cheng (Eds.) *Handbook of Thermal Analysis and Calorimetry*, Elsevier, **2002**, *3*, 49.

[16] G.B. McKenna, S.L. Simon, *Macromolecules.* **2017**, *50*, 6333.

[17] C.B. Roth, ed., *Polymer Glasses*, CRC Press, **2016**.

[18] D. Cangialosi, *J. Phys. Condens. Matter*. **2014**, *26*, 153101.

[19] T.P. Russell, Y. Chai, *Macromolecules.* **2017**, *50*, 4597.

[20] R.D. Priestley, D. Cangialosi, S. Napolitano, *J. Non. Cryst. Solids*. **2015**, *407*, 288.

[21] S. Napolitano, E. Glynos, N.B. Tito, *Reports Prog. Phys.* **2017**, *80*, 36602.

[22] K.L. Ngai, *The glass transition and the glassy state, in Physical Properties of Polymers*, 3rd Edition, Cambridge University Press, **2004**.

[23] A.V. Tobolsky, *Properties and structure of polymers*, John Wiley & Sons, Inc., **1960**.

[24] A. V Tobolsky, *J. Polym. Sci. Part C Polym. Symp.* **1965**, *9*, 157.

[25] R. Xie, Y. Lee, M.P. Aplan, N.J. Caggiano, C. Müller, R.H. Colby, E.D. Gomez, *Macromolecules*. **2017**, *50*, 5146.

[26] T. Alfrey, G. Goldfinger, H. Mark, *J. Appl. Phys.* **1943**, *14*, 700.

[27] M.J. Richardson, N.G. Savill, *Polymer*. **1975**, *16*, 753.

[28] C.T. Moynihan, A.J. Easteal, M.A. De Bolt, J. Tucker, *J. Am. Ceram. Soc.* **1976**, *59*, 12.

[29] S. Gao, S.L. Simon, *Thermochim. Acta*. **2015**, *603*, 123.

[30] J.D. Ferry, *Viscoelastic Properties of Polymers*, 3rd ed., John Wiley & Sons, Inc., **1980**.

[31] R. Greiner, F.R. Schwarzl, *Rheol. Acta*. **1984**, *23*, 378.

[32] Y.P. Koh, S.L. Simon, *J. Polym. Sci. Part B Polym. Phys.* **2008**, *46*, 2741.

[33] Z. Qian, J. Risan, B. Stadnick, G.B. McKenna, *J. Polym. Sci. Part B Polym. Phys.* **2018**, *56*, 414.

[34] M. Alcoutlabi, G.B. McKenna, *J. Phys. Condens. Matter*. **2005**, *17*, R461.

[35] P. Zoller, Dilatometry, in: *Encyclopedia of Polymer Science and Technology* **2013**.

[36] A.J. Batschinski, *Zeitschrift Für Phys. Chemie*. **1913**, *84U*, 643.

[37] D.B. Macleod, *Trans. Faraday Soc.* **1923**, *19*, 6.

[38] T.G. Fox, P.J. Flory, *J. Appl. Phys.* **1950**, *21*, 581.

[39] A.K. Doolittle, *J. Appl. Phys.* **1951**, *22*, 1471.

[40] R.P. White, J.E.G. Lipson, *Macromolecules*. **2016**, *49*, 3987.

[41] T.G. Fox, P.J. Flory, *J. Polym. Sci.* **1954**, *14*, 315.

[42] M.L. Williams, R.F. Landel, J.D. Ferry, *J. Am. Chem. Soc.* **1955**, *77*, 3701.

[43] H. Vogel, *Phys. Zeitschrift*. **1921**, *22*, 645.

[44] G.S. Fulcher, *J. Am. Ceram. Soc.* **1925**, *8*, 339.

[45] G. Tammann, W. Hesse, *Zeitschrift Für Anorg. Und Allg. Chemie*. **1926**, *156*, 245.

[46] J.H. Gibbs, E.A. DiMarzio, *J. Chem. Phys.* **1958**, *28*, 373.

[47] E.A. DiMarzio, J.H. Gibbs, *J. Chem. Phys.* **1958**, *28*, 807.

[48] P.J. Flory, *Principles of Polymer Chemistry*, Cornell University Press, **1953**,.

[49] M.L. Huggins, *Ann. N. Y. Acad. Sci.* **1942**, *43*, 1.

[50] W. Kauzmann, *Chem. Rev.* **1948**, *43*, 219.

[51] G. Adam, J.H. Gibbs, *J. Chem. Phys.* **1965**, *43*, 139.

[52] J. Moacanin, R. Simha, *J. Chem. Phys.* **1966**, *45*, 964.

[53] J.M.G. Cowie, V. Arrighi, *Polymers: Chemistry and Physics of Modern Materials*, 3rd ed., CRC Press, **2007**,.

[54] F.N. Kelley, F. Bueche, *J. Polym. Sci.* **1961**, *50*, 549.

[55] F. Bueche, *Physical properties of polymers*, Interscience Publishers, **1962**,.

[56] G. Pezzin, F. Zilio-Grandi, P. Sanmartin, *Eur. Polym. J.* **1970**, *6*, 1053.

[57] R.B. Beevers, E.F.T. White, *Trans. Faraday Soc.* **1960**, *56*, 744.

[58] J.M.G. Cowie, P.M. Toporowski, *Eur. Polym. J.* **1968**, *4*, 621.

[59] R.F. Boyer, *Rubber Chem. Technol.* **1963**, *36*, 1303.

[60] M.C. Shen, A. Eisenberg, *Rubber Chem. Technol.* **1970**, *43*, 95.

[61] V.P. Privalko, Y.S. Lipatov, *J. Macromol. Sci. Part B.* **1974**, *9*, 551.

[62] K.K. Chee, *J. Appl. Polym. Sci.* **1991**, *43*, 1205.

[63] J. Dudowicz, K.F. Freed, J.F. Douglas, *J. Phys. Chem. B.* **2005**, *109*, 21285.

[64] P.C. Painter, M.M. Coleman, *Fundamentals of Polymer Science: An Introductory Text*, 2nd ed., CRC Press, **1997**.

[65] J.L. Halary, F. Lauprêtre, L. Monnerie, *Polymer Materials: Macroscopic Properties and Molecular Interpretations*, John Wiley & Sons, Inc., **2011**,.

[66] B. Wunderlich, *Prog. Polym. Sci.* **2003**, *28*, 383.

[67] H. Suzuki, J. Grebowicz, B. Wunderlich, *Br. Polym. J.* **1985**, *17*, 1.

[68] J. Martín, N. Stingelin, D. Cangialosi, *J. Phys. Chem. Lett.* **2018**, *9*, 990.

[69] C.L. Jackson, G.B. McKenna, *J. Non. Cryst. Solids.* **1991**, *131–133*, 221.

[70] B.D. Vogt, *J. Polym. Sci. Part B Polym. Phys.* **2018**, *56*, 9.

[71] D. Cangialosi, *Chapter 8 - Glass Transition and Physical Aging of Confined Polymers Investigated by Calorimetric Techniques*, in: S. Vyazovkin, N. Koga, C. Schick (Eds.) *Handbook of Thermal Analysis and Calorimetry*, Elsevier, **2018**, *6*, 301.

[72] J.H. Mangalara, M.E. Mackura, M.D. Marvin, D.S. Simmons, *J. Chem. Phys.* **2017**, *146*, 203316.

[73] W. Zhang, J.F. Douglas, F.W. Starr, *Proc. Natl. Acad. Sci.* **2018**, *115*, 5641.

[74] W. Zhang, J.F. Douglas, F.W. Starr, *AIP Conf. Proc.* **2018**, *1981*, 20083.

[75] J.L. Keddie, R.A.L. Jones, R.A. Cory, *Europhys. Lett.* **1994**, *27*, 59.

[76] J.A. Forrest, K. Dalnoki-Veress, *Adv. Colloid Interface Sci.* **2001**, *94*, 167.

[77] C.B. Roth, J.R. Dutcher, *J. Electroanal. Chem.* **2005**, *584*, 13.

[78] M.D. Ediger, J.A. Forrest, *Macromolecules*. **2014**, *47*, 471.

[79] F. Kremer, M. Tress, E.U. Mapesa, *J. Non. Cryst. Solids*. **2015**, *407*, 277.

[80] D. Cangialosi, A. Alegría, J. Colmenero, *Prog. Polym. Sci.* **2016**, *54–55*, 128.

[81] K. Fukao, Y. Miyamoto, *Europhys. Lett.* **1999**, *46*, 649.

[82] K. Fukao, Y. Miyamoto, *Phys. Rev. E.* **2000**, *61*, 1743.

[83] K. Fukao, *Eur. Phys. J. E.* **2003**, *12*, 119.

[84] R.D. Priestley, L.J. Broadbelt, J.M. Torkelson, K. Fukao, *Phys. Rev. E.* **2007**, *75*, 61806.

[85] H. Yin, D. Cangialosi, A. Schönhals, *Thermochim. Acta*. **2013**, *566*, 186.

[86] X. Wang, W. Zhou, *Macromolecules*. **2002**, *35*, 6747.

[87] M.Y. Efremov, J.T. Warren, E.A. Olson, M. Zhang, A.T. Kwan, L.H. Allen, *Macromolecules*. **2002**, *35*, 1481.

[88] J.L. Keddie, R.A.L. Jones, R.A. Cory, *Faraday Discuss.* **1994**, *98*, 219.

[89] D.S. Fryer, P.F. Nealey, J.J. de Pablo, *Macromolecules*. **2000**, *33*, 6439.

[90] G.B. DeMaggio, W.E. Frieze, D.W. Gidley, M. Zhu, H.A. Hristov, A.F. Yee, *Phys. Rev. Lett.* **1997**, *78*, 1524.

[91] J.A. Forrest, K. Dalnoki-Veress, J.R. Dutcher, A.C. Rowat, J.R. Stevens, *MRS Proc.* **1995**, *407*, 131.

[92] J.A. Forrest, K. Dalnoki-Veress, J.R. Stevens, J.R. Dutcher, *Phys. Rev. Lett.* **1996**, *77*, 2002.

[93] J.A. Forrest, K. Dalnoki-Veress, J.R. Dutcher, *Phys. Rev. E.* **1997**, *56*, 5705.

[94] K. Dalnoki-Veress, J.A. Forrest, C. Murray, C. Gigault, J.R. Dutcher, *Phys. Rev. E.* **2001**, *63*, 31801.

[95] Z. Fakhraai, J.A. Forrest, *Phys. Rev. Lett.* **2005**, *95*, 25701.

[96] M.Y. Efremov, A. V Kiyanova, P.F. Nealey, *Macromolecules*. **2008**, *41*, 5978.

[97] M.Y. Efremov, A. V Kiyanova, J. Last, S.S. Soofi, C. Thode, P.F. Nealey, *Phys. Rev. E.* **2012**, *86*, 21501.

[98] C.J. Ellison, J.M. Torkelson, *J. Polym. Sci. Part B Polym. Phys.* **2002**, *40*, 2745.

[99] G. Reiter, *EPL (Europhysics Lett.* **1993**, *23*, 579.

[100] J. Wang, G.B. McKenna, *Macromolecules*. **2013**, *46*, 2485.

[101] X. Li, G.B. McKenna, *Macromolecules*. **2015**, *48*, 6329.

[102] J. Wang, G.B. McKenna, *J. Polym. Sci. Part B Polym. Phys.* **2013**, *51*, 1343.

[103] J.H. Teichroeb, J.A. Forrest, *Phys. Rev. Lett.* **2003**, *91*, 16104.

[104] P.A. O'Connell, S.A. Hutcheson, G.B. McKenna, Rheological Measurements at the Nanoscale: Creep Compliance Measurements in Thin Films and at Surfaces, in: Proc. World Polym. Congr. Macro 2004., Paris, **2004**.

[105] S.A. Hutcheson, G.B. McKenna, *Phys. Rev. Lett.* **2005**, *94*, 76103.

[106] Z. Fakhraai, J.A. Forrest, *Science.* **2008**, *319*, 600.

[107] H. Yoon, G.B. McKenna, *Macromolecules*. **2014**, *47*, 8808.

[108] P.A. O'Connell, G.B. McKenna, *Science.* **2005**, *307*, 1760.

[109] P.A. O'Connell, G.B. McKenna, *Rev. Sci. Instrum.* **2007**, *78*, 13901.

[110] P.A. O'Connell, G.B. McKenna, *Eur. Phys. J. E.* **2006**, *20*, 143.

[111] P.A. O'Connell, S.A. Hutcheson, G.B. McKenna, *J. Polym. Sci. Part B Polym. Phys.* **2008**, *46*, 1952.

[112] P.A. O'Connell, J. Wang, T.A. Ishola, G.B. McKenna, *Macromolecules*. **2012**, *45*, 2453.

[113] J.S. Sharp, J.A. Forrest, *Eur. Phys. J. E.* **2003**, *12*, 97.

[114] C.B. Roth, J.R. Dutcher, *Eur. Phys. J. E.* **2003**, *12*, 103.

[115] M. Tress, M. Erber, E.U. Mapesa, H. Huth, J. Müller, A. Serghei, C. Schick, K.-J. Eichhorn, B. Voit, F. Kremer, *Macromolecules*. **2010**, *43*, 9937.

[116] J.W. Schultz, *Encycl. Anal. Chem.* **2006**,.

[117] F. Kremer, A. Schönhals, eds., *Broadband Dielectric Spectroscopy*, Springer-Verlag Berlin Heidelberg, **2003**.

[118] S. Havriliak, S. Negami, *J. Polym. Sci. Part C Polym. Symp.* **1966**, *14*, 99.

[119] P. Ben Ishai, M.S. Talary, A. Caduff, E. Levy, Y. Feldman, *Meas. Sci. Technol.* **2013**, *24*, 102001.

[120] A. Alegria, J. Colmenero, *Soft Matter*. **2016**, *12*, 7709.

[121] M. Mierzwa, G. Floudas, M. Neidhöfer, R. Graf, H.W. Spiess, W.H. Meyer, G. Wegner, *J. Chem. Phys.* **2002**, *117*, 6289.

[122] P. Papadopoulos, G. Floudas, C. Chi, G. Wegner, *J. Chem. Phys.* **2004**, *120*, 2368.

[123] A. Gitsas, G. Floudas, G. Wegner, *Phys. Rev. E.* **2004**, *69*, 41802.

[124] P.E. Hopkinson, P.A. Staniec, A.J. Pearson, A.D.F. Dunbar, T. Wang, A.J. Ryan, R.A.L. Jones, D.G. Lidzey, A.M. Donald, *Macromolecules*. **2011**, *44*, 2908.

[125] B.C. Schroeder, Y.-C. Chiu, X. Gu, Y. Zhou, J. Xu, J. Lopez, C. Lu, M.F. Toney, Z. Bao, *Adv. Electron. Mater.* **2016**, *2*, 1600104.

[126] A. Sharma, X. Pan, J.A. Campbell, M.R. Andersson, D.A. Lewis, *Macromolecules*. **2017**, *50*, 3347.

[127] R. Xie, R.H. Colby, E.D. Gomez, *Adv. Electron. Mater.* **2018**, *4*, 1700356.

[128] Q. Li, S.A. Hutcheson, G.B. McKenna, S.L. Simon, *J. Polym. Sci. Part B Polym. Phys.* **2008**, *46*, 2719.

[129] S. Pankaj, E. Hempel, M. Beiner, *Macromolecules*. **2009**, *42*, 716.

[130] M. Hu, Y. Xia, G.B. McKenna, J.A. Kornfield, R.H. Grubbs, *Macromolecules*. **2011**, *44*, 6935.

[131] M. Hu, Y. Xia, C.S. Daeffler, J. Wang, G.B. McKenna, J.A. Kornfield, R.H. Grubbs, *J. Polym. Sci. Part B Polym. Phys.* **2015**, *53*, 899.

[132] Z. Qian, Y.P. Koh, M.R. Pallaka, A.B. Chang, T.-P. Lin, P.E. Guzmán, R.H. Grubbs, S.L. Simon, G.B. McKenna, *Macromolecules*. n.d. Under Review.

[133] Z. Qian, Ph.D. Thesis, Viscoelastic and Nanomechanical Behaviors of Polymeric Materials, Texas Tech University, August, **2018**.

[134] A.A.Y. Guilbert, A. Urbina, J. Abad, C. Díaz-Paniagua, F. Batallán, T. Seydel, M. Zbiri, V. García-Sakai, J. Nelson, *Chem. Mater.* **2015**, *27*, 7652.

[135] P. Zhan, W. Zhang, I.E. Jacobs, D.M. Nisson, R. Xie, A.R. Weissen, R.H. Colby, A.J. Moulé, S.T. Milner, J.K. Maranas, E.D. Gomez, *J. Polym. Sci. Part B Polym. Phys.* **2018**, *56*, 1193.

[136] P.J. Haines, M. Reading, F.W. Wilburn, *Chapter 5 - Differential Thermal Analysis and Differential Scanning Calorimetry*, in: M. E. Brown (Eds.) *Handbook of Thermal Analysis and Calorimetry*, Elsevier Science B.V., **1998**, *1*, 279.

[137] D.J. Plazek, Z.N. Frund Jr., *J. Polym. Sci. Part B Polym. Phys.* **1990**, *28*, 431.

[138] D.J. Plazek, K.L. Ngai, *The Glass Temperature*, in: *Physical Properties of Polymer Handbook*, J.E. Mark (Ed.), 2nd Edition, Springer New York, New York, NY, **2007**.

[139] P. Badrinarayanan, W. Zheng, Q. Li, S.L. Simon, *J. Non. Cryst. Solids*. **2007**, *353*, 2603.

[140] A.Q. Tool, *J. Am. Ceram. Soc.* **1946**, *29*, 240.

[141] Y.P. Koh, G.B. McKenna, S.L. Simon, *J. Polym. Sci. Part B Polym. Phys.* **2006**, *44*, 3518.

[142] K. Fukao, T. Terasawa, Y. Oda, K. Nakamura, D. Tahara, *Phys. Rev. E*. **2011**, *84*, 41808.

[143] D.S. Langhe, T.M. Murphy, A. Shaver, C. LaPorte, B.D. Freeman, D.R. Paul, E. Baer, *Polymer*. **2012**, *53*, 1925.

[144] V.M. Boucher, D. Cangialosi, H. Yin, A. Schönhals, A. Alegría, J. Colmenero, *Soft Matter*. **2012**, *8*, 5119.

[145] V.M. Boucher, D. Cangialosi, A. Alegría, J. Colmenero, *Phys. Chem. Chem. Phys.* **2017**, *19*, 961.

[146] E.A. Olson, M.Y. Efremov, M. Zhang, Z. Zhang, L.H. Allen, *J. Microelectromechanical Syst.* **2003**, *12*, 355.

[147] M.Y. Efremov, E.A. Olson, M. Zhang, Z. Zhang, L.H. Allen, *Phys. Rev. Lett.* **2003**, *91*, 85703.

[148] M.Y. Efremov, E.A. Olson, M. Zhang, L.H. Allen, *Thermochim. Acta.* **2003**, *403*, 37.

[149] M.Y. Efremov, E.A. Olson, M. Zhang, Z. Zhang, L.H. Allen, *Macromolecules.* **2004**, *37*, 4607.

[150] M.Y. Efremov, E.A. Olson, M. Zhang, F. Schiettekatte, Z. Zhang, L.H. Allen, *Rev. Sci. Instrum.* **2004**, *75*, 179.

[151] A.W. van Herwaarden, *Thermochim. Acta.* **2005**, *432*, 192.

[152] A.A. Minakov, S.A. Adamovsky, C. Schick, *Thermochim. Acta.* **2005**, *432*, 177.

[153] H. Huth, A.A. Minakov, C. Schick, *J. Polym. Sci. Part B Polym. Phys.* **2006**, *44*, 2996.

[154] H. Huth, A.A. Minakov, A. Serghei, F. Kremer, C. Schick, *Eur. Phys. J. Spec. Top.* **2007**, *141*, 153.

[155] D. Zhou, H. Huth, Y. Gao, G. Xue, C. Schick, *Macromolecules.* **2008**, *41*, 7662.

[156] S. Luo, Y. Chen, Y. Sha, G. Xue, E. Zhuravlev, C. Schick, X. Wang, D. Zhou, L. Li, *Polymer.* **2018**, *134*, 204.

[157] Y.P. Koh, L. Grassia, S.L. Simon, *Thermochim. Acta.* **2015**, *603*, 135.

[158] C. Schick, V. Mathot, eds., *Fast Scanning Calorimetry*, Springer International Publishing, **2016**.

[159] E. Lopez, S.L. Simon, *Macromolecules.* **2016**, *49*, 2365.

[160] H. Yoon, Y.P. Koh, S.L. Simon, G.B. McKenna, *Macromolecules.* **2017**, *50*, 4562.

[161] N.G. Perez-de-Eulate, V. Di Lisio, D. Cangialosi, *ACS Macro Lett.* **2017**, *6*, 859.

[162] Y.P. Koh, S.L. Simon, *J. Chem. Phys.* **2017**, *146*, 203329.

[163] S. Luo, L. Wei, J. Jiang, Y. Sha, G. Xue, X. Wang, D. Zhou, *J. Polym. Sci. Part B Polym. Phys.* **2017**, *55*, 1357.

[164] S. Luo, X. Kui, E. Xing, X. Wang, G. Xue, C. Schick, W. Hu, E. Zhuravlev, D. Zhou, *Macromolecules.* **2018**, *51*, 5209.

[165] S. Zhang, M.U. Ocheje, S. Luo, D. Ehlenberg, B. Appleby, D. Weller, D. Zhou, S. Rondeau-Gagné, X. Gu, *Macromol. Rapid Commun.* **2018**, *39*, 1800092.

[166] C. Schick, R. Androsch, Chapter 2 - Fast Scanning Chip Calorimetry, in: S. Vyazovkin, N. Koga, C. Schick (Eds.) *Handbook of Thermal Analysis and Calorimetry*, Elsevier Science

B.V., **2018**, *6*, 47.

[167] Y.P. Koh, S.L. Simon, *Polymer*. **2018**, *143*, 40.

[168] L. Grassia, Y.P. Koh, M. Rosa, S.L. Simon, *Macromolecules*. **2018**, *51*, 1549.

[169] J. Chen, J. Xu, X. Wang, D. Zhou, P. Sun, G. Xue, *Macromolecules*. **2013**, *46*, 7006.

[170] J. Chen, L. Li, D. Zhou, J. Xu, G. Xue, *Macromolecules*. **2014**, *47*, 3497.

[171] A.A. Minakov, A.W. van Herwaarden, W. Wien, A. Wurm, C. Schick, *Thermochim. Acta*. **2007**, *461*, 96.

[172] E. Zhuravlev, C. Schick, *Thermochim. Acta*. **2010**, *505*, 1.

[173] E. Zhuravlev, C. Schick, *Thermochim. Acta*. **2010**, *505*, 14.

[174] I. Kolesov, D. Mileva, R. Androsch, C. Schick, *Polymer*. **2011**, *52*, 5156.

[175] S. Gao, Y.P. Koh, S.L. Simon, *Macromolecules*. **2013**, *46*, 562.

[176] N. Shamim, Y.P. Koh, S.L. Simon, G.B. McKenna, *J. Polym. Sci. Part B Polym. Phys.* **2014**, *52*, 1462.

[177] J.E.K. Schawe, *Thermochim. Acta*. **2015**, *603*, 128.

[178] C.M. Roland, P.G. Santangelo, K.L. Ngai, *J. Chem. Phys.* **1999**, *111*, 5593.

[179] C.R. Snyder, D.M. DeLongchamp, *Curr. Opin. Solid State Mater. Sci.* **2018**, *22*, 41.

[180] E. Donth, *J. Polym. Sci. Part B Polym. Phys.* **1996**, *34*, 2881.

[181] M. Pyda, A. Boller, J. Grebowicz, H. Chuah, B. V. Lebedev, B. Wunderlich, *J. Polym. Sci. Part B Polym. Phys.* **1998**, *36*, 2499.

[182] J.D. Menczel, R.B. Prime, eds., *Thermal analysis of polymers: fundamentals and applications*, John Wiley & Sons, **2009**.

[183] J. Yao, C. Yu, Z. Liu, H. Luo, Y. Yang, G. Zhang, D. Zhang, *J. Am. Chem. Soc.* **2016**, *138*, 173.

[184] A. Zhang, C. Xiao, Y. Wu, C. Li, Y. Ji, L. Li, W. Hu, Z. Wang, W. Ma, W. Li, *Macromolecules*. **2016**, *49*, 6431.

[185] S. Chen, B. Sun, W. Hong, H. Aziz, Y. Meng, Y. Li, *J. Mater. Chem. C*. **2014**, *2*, 2183.

[186] H. Yu, K.H. Park, I. Song, M.-J. Kim, Y.-H. Kim, J.H. Oh, *J. Mater. Chem. C*. **2015**, *3*, 11697.

[187] J. Zhao, A. Swinnen, G. Van Assche, J. Manca, D. Vanderzande, B. Van Mele, *J. Phys. Chem. B.* **2009**, *113*, 1587.

[188] J. Zhao, S. Bertho, J. Vandenbergh, G. Van Assche, J. Manca, D. Vanderzande, X. Yin, J. Shi, T. Cleij, L. Lutsen, B. Van Mele, *Phys. Chem. Chem. Phys.* **2011**, *13*, 12285.

[189] G. Beaucage, R. Composto, R.S. Stein, *J. Polym. Sci. Part B Polym. Phys.* **1993**, *31*, 319.

[190] W.J. Orts, J.H. van Zanten, W. Wu, S.K. Satija, *Phys. Rev. Lett.* **1993**, *71*, 867.

[191] W.E. Wallace, J.H. van Zanten, W.L. Wu, *Phys. Rev. E.* **1995**, *52*, R3329.

[192] D.J. Pochan, E.K. Lin, S. Satija, S.Z.D. Cheng, W.-L. Wu, *MRS Proc.* **1998**, *543*, 163.

[193] D.J. Pochan, E.K. Lin, S.K. Satija, W. Wu, *Macromolecules.* **2001**, *34*, 3041.

[194] M. Campoy-Quiles, P.G. Etchegoin, D.D.C. Bradley, *Synth. Met.* **2005**, *155*, 279.

[195] M. Campoy-Quiles, M. Sims, P.G. Etchegoin, D.D.C. Bradley, *Macromolecules.* **2006**, *39*, 7673.

[196] C. Müller, J. Bergqvist, K. Vandewal, K. Tvingstedt, A.S. Anselmo, R. Magnusson, M.I. Alonso, E. Moons, H. Arwin, M. Campoy-Quiles, O. Inganäs, *J. Mater. Chem.* **2011**, *21*, 10676.

[197] T. Wang, A.J. Pearson, A.D.F.F. Dunbar, P.A. Staniec, D.C. Watters, D. Coles, H. Yi, A. Iraqi, D.G. Lidzey, R.A.L.L. Jones, *Eur. Phys. J. E.* **2012**, *35*, 2.

[198] A.J. Pearson, T. Wang, R.A.L. Jones, D.G. Lidzey, P.A. Staniec, P.E. Hopkinson, A.M. Donald, *Macromolecules.* **2012**, *45*, 1499.

[199] T. Wang, A.J. Pearson, A.D.F. Dunbar, P.A. Staniec, D.C. Watters, H. Yi, A.J. Ryan, R.A.L. Jones, A. Iraqi, D.G. Lidzey, *Adv. Funct. Mater.* **2012**, *22*, 1399.

[200] C. Müller, L.M. Andersson, O. Peña-Rodríguez, M. Garriga, O. Inganäs, M. Campoy-Quiles, *Macromolecules.* **2013**, *46*, 7325.

[201] D. Liu, R. Osuna Orozco, T. Wang, *Phys. Rev. E.* **2013**, *88*, 22601.

[202] D. Liu, H. Qin, J. Zhang, T. Wang, *Phys. Rev. E.* **2016**, *94*, 52503.

[203] C. Langhammer, E.M. Larsson, B. Kasemo, I. Zorić, *Nano Lett.* **2010**, *10*, 3529.

[204] F.A.A. Nugroho, A. Diaz de Zerio Mendaza, C. Lindqvist, T.J. Antosiewicz, C. Müller, C. Langhammer, *Anal. Chem.* **2017**, *89*, 2575.

[205] A. Diaz de Zerio Mendaza, A. Melianas, F.A.A. Nugroho, O. Bäcke, E. Olsson, C. Langhammer, O. Inganäs, C. Müller, *J. Mater. Chem. A.* **2017**, *5*, 4156.

[206] S.E. Root, M.A. Alkhadra, D. Rodriquez, A.D. Printz, D.J. Lipomi, *Chem. Mater.* **2017**, *29*, 2646.

[207] C. Müller, *Chem. Mater.* **2015**, *27*, 2740.

[208] C. Lu, W.Y. Lee, X. Gu, J. Xu, H.H. Chou, H. Yan, Y.C. Chiu, M. He, J.R. Matthews, W. Niu, J.B.H. Tok, M.F. Toney, W.C. Chen, Z. Bao, *Adv. Electron. Mater.* **2017**, *3*, 1600311.

[209] H. Koezuka, A. Tsumura, T. Ando, *Synth. Met.* **1987**, *18*, 699.

[210] A. Assadi, C. Svensson, M. Willander, O. Inganäs, *Appl. Phys. Lett.* **1988**, *53*, 195.

[211] Z. Bao, A. Dodabalapur, A.J. Lovinger, *Appl. Phys. Lett.* **1996**, *69*, 4108.

[212] T.A. Chen, R.D. Rieke, *J. Am. Chem. Soc.* **1992**, *114*, 10087.

[213] R.D. McCullough, R.D. Lowe, *J. Chem. Soc. Chem. Commun.* **1992**, 70.

[214] S. Savagatrup, A.D. Printz, D. Rodriquez, D.J. Lipomi, *Macromolecules*. **2014**, *47*, 1981.

[215] S.-A.A. Chen, J.-M.M. Ni, *Macromolecules*. **1992**, *25*, 6081.

[216] S. Pankaj, M. Beiner, *J. Phys. Chem. B.* **2010**, *114*, 15459.

[217] L. Yu, E. Davidson, A. Sharma, M.R. Andersson, R. Segalman, C. Müller, *Chem. Mater.* **2017**, *29*, 5654.

[218] I. McCulloch, M. Heeney, C. Bailey, K. Genevicius, I. MacDonald, M. Shkunov, D. Sparrowe, S. Tierney, R. Wagner, W. Zhang, M.L. Chabinyc, R.J. Kline, M.D. McGehee, M.F. Toney, *Nat. Mater.* **2006**, *5*, 328.

[219] B. O'Connor, E.P. Chan, C. Chan, B.R. Conrad, L.J. Richter, R.J. Kline, M. Heeney, I. McCulloch, C.L. Soles, D.M. DeLongchamp, *ACS Nano*. **2010**, *4*, 7538.

[220] R.J. Kline, D.M. DeLongchamp, D.A. Fischer, E.K. Lin, L.J. Richter, M.L. Chabinyc, M.F. Toney, M. Heeney, I. McCulloch, *Macromolecules*. **2007**, *40*, 7960.

[221] J. Mei, Z. Bao, *Chem. Mater*. **2014**, *26*, 604.

[222] M. Leclerc, *J. Polym. Sci. Part A Polym. Chem*. **2001**, *39*, 2867.

[223] J. Teetsov, M. Anne Fox, *Polymer*. **1999**, *9*, 2117.

[224] A. Donat-Bouillud, I. Lévesque, Y. Tao, M. D'Iorio, S. Beaupré, P. Blondin, M. Ranger, J. Bouchard, M. Leclerc, *Chem. Mater.* **2000**, *12*, 1931.

[225] L. Kinder, J. Kanicki, P. Petroff, *Synth. Met*. **2004**, *146*, 181.

[226] S.K.H. Wei, L. Zeng, K.L. Marshall, S.H. Chen, W.S. K.-H., Z. Lichang, M.K. L., C.S. H., *J. Polym. Sci. Part B Polym. Phys.* **2011**, *49*, 725.

[227] M.J. Banach, R.H. Friend, H. Sirringhaus, *Macromolecules*. **2003**, *36*, 2838.

[228] C. Müller, E. Wang, L.M. Andersson, K. Tvingstedt, Y. Zhou, M.R. Andersson, O. Inganäs, *Adv. Funct. Mater.* **2010**, *20*, 2124.

[229] C. Müller, M. Esmaeili, C. Riekel, D.W. Breiby, O. Inganäs, *Polymer*. **2013**, *54*, 805.

[230] R. Xie, M.P. Aplan, N.J. Caggiano, A.R. Weisen, T. Su, C. Müller, M. Segad, R.H. Colby, E.D. Gomez, *Macromolecules*. **2018**, *51*, 10271.

[231] R. Kroon, *CHALMERS Univ. Technol.* **2013**,.

[232] M. Shakutsui, H. Matsuura, K. Fujita, *Org. Electron. Physics, Mater. Appl.* **2009**, *10*, 834.

[233] S.H. Chen, A.C. Su, C.H. Su, S.A. Chen, *J. Phys. Chem. B.* **2006**, *110*, 4007.

[234] P. Blondin, J. Bouchard, S. Beaupré, M. Belletête, G. Durocher, M. Leclerc, *Macromolecules*. **2000**, *33*, 5874.

[235] B. Tanto, S. Guha, C.M. Martin, U. Scherf, M.J. Winokur, *Macromolecules*. **2004**, *37*, 9438.

[236] A.J. Heeger, *Adv*. *Mater*. **2014**, *26*, 10.

[237] H. Sirringhaus, *Adv*. *Mater*. **2014**, *26*, 1319.

[238] J. Sun, Y. Zhu, X. Xu, L. Lan, L. Zhang, P. Cai, J. Chen, J. Peng, Y. Cao, *J. Phys. Chem. C*. **2012**, *116*, 14188.

[239] E. Wang, L. Hou, Z. Wang, Z. Ma, S. Hellström, W. Zhuang, F. Zhang, O. Inganäs, M.R. Andersson, *Macromolecules*. **2011**, *44*, 2067.

[240] W. Zhang, J. Smith, S.E. Watkins, R. Gysel, M. McGehee, A. Salleo, J. Kirkpatrick, S. Ashraf, T. Anthopoulos, M. Heeney, I. McCulloch, *J. Am. Chem. Soc.* **2010**, *132*, 11437.

[241] Y. Li, W.K. Tatum, J.W. Onorato, Y. Zhang, C.K. Luscombe, *Macromolecules*. **2018**, *51*, 6352.

[242] J. Yin, W. Zhou, L. Zhang, Y. Xie, Z. Yu, J. Shao, W. Ma, J. Zeng, Y. Chen, *Macromol. Rapid Commun.* **2017**, *38*, 1.

[243] S.E. Root, N.E. Jackson, S. Savagatrup, G. Arya, D.J. Lipomi, *Energy Environ. Sci.* **2017**, *10*, 558.

[244] J. Kesters, P. Verstappen, J. Raymakers, W. Vanormelingen, J. Drijkoningen, J. D'Haen, J. Manca, L. Lutsen, D. Vanderzande, W. Maes, J. D'Haen, J. Manca, L. Lutsen, D. Vanderzande, W. Maes, *Chem. Mater.* **2015**, *27*, 1332.

[245] T.-Y. Chu, J. Lu, S. Beaupré, Y. Zhang, J.-R. Pouliot, J. Zhou, A. Najari, M. Leclerc, Y. Tao, *Adv. Funct. Mater.* **2012**, *22*, 2345.

[246] L. Biniek, B.C. Schroeder, C.B. Nielsen, I. McCulloch, *J. Mater. Chem.* **2012**, *22*, 14803.

[247] Z. Yi, S. Wang, Y. Liu, *Adv. Mater.* **2015**, *27*, 3589.

[248] N.E. Jackson, B.M. Savoie, K.L. Kohlstedt, M. Olvera De La Cruz, G.C. Schatz, L.X. Chen, M.A. Ratner, *J. Am. Chem. Soc.* **2013**, *135*, 10475.

[249] J.C. Bijleveld, A.P. Zoombelt, S.G.J. Mathijssen, M.M. Wienk, M. Turbiez, D.M. de Leeuw, R.A.J. Janssen, *J. Am. Chem. Soc.* **2009**, *131*, 16616.

[250] Y. Li, S.P. Singh, P. Sonar, *Adv. Mater.* **2010**, *22*, 4862.

[251] X. Zhang, L.J. Richter, D.M. DeLongchamp, R.J. Kline, M.R. Hammond, I. McCulloch, M. Heeney, R.S. Ashraf, J.N. Smith, T.D. Anthopoulos, B. Schroeder, Y.H. Geerts, D.A. Fischer, M.F. Toney, *J. Am. Chem. Soc.* **2011**, *133*, 15073.

[252] C. Cheng, C. Yu, Y. Guo, H. Chen, Y. Fang, G. Yu, Y. Liu, *Chem. Commun.* **2013**, *49*, 1998.

[253] T.L. Nelson, T.M. Young, J. Liu, S.P. Mishra, J.A. Belot, C.L. Balliet, A.E. Javier, T. Kowalewski, R.D. McCullough, *Adv. Mater.* **2010**, *22*, 4617.

[254] J.C. Bijleveld, V.S. Gevaerts, D. Di Nuzzo, M. Turbiez, S.G.J. Mathijssen, D.M. de Leeuw, M.M. Wienk, R.A.J. Janssen, *Adv. Mater.* **2010**, *22*, E242.

[255] P. Sonar, S.P. Singh, Y. Li, M.S. Soh, A. Dodabalapur, *Adv. Mater.* **2010**, *22*, 5409.

[256] S. Zhang, M.U. Ocheje, L. Huang, L. Galuska, Z. Cao, S. Luo, Y.-H. Cheng, D. Ehlenberg, R.B. Goodman, D. Zhou, Y. Liu, Y.-C. Chiu, J.D. Azoulay, S. Rondeau-Gagné, X. Gu, *Adv. Electron. Mater.* Under Review.

[257] J. Mei, K.R. Graham, R. Stalder, J.R. Reynolds, *Org. Lett.* **2010**, *12*, 660.

[258] T. Lei, Y. Cao, Y. Fan, C.-J. Liu, S.-C. Yuan, J. Pei, *J. Am. Chem. Soc.* **2011**, *133*, 6099.

[259] T. Lei, J.-H. Dou, J. Pei, *Adv. Mater.* **2012**, *24*, 6457.

[260] Y. Yang, R. Wu, X. Wang, X. Xu, Z. Li, K. Li, Q. Peng, *Chem. Commun.* **2014**, *50*, 439.

[261] B. Fu, J. Baltazar, A.R. Sankar, P.-H. Chu, S. Zhang, D.M. Collard, E. Reichmanis, *Adv. Funct. Mater.* **2014**, *24*, 3734.

[262] B.C. Schroeder, T. Kurosawa, T. Fu, Y.-C. Chiu, J. Mun, G.-J.N. Wang, X. Gu, L. Shaw, J.W.E. Kneller, T. Kreouzis, M.F. Toney, Z. Bao, *Adv. Funct. Mater.* **2017**, *27*, 1701973.

[263] J.H. Burroughes, D.D.C. Bradley, A.R. Brown, R.N. Marks, K. Mackay, R.H. Friend, P.L. Burns, A.B. Holmes, *Nature*. **1990**, *347*, 539.

[264] T.W. Lee, O.O. Park, *Adv. Mater.* **2000**, *12*, 801.

[265] J.Y. Kim, C.D. Frisbie, *J. Phys. Chem. C*. **2008**, *112*, 17726.

[266] Y. Liu, H. Ma, A.K.Y. Jen, *Chem. Commun.* **1998**, *95*, 2747.

[267] O. Schäfer, A. Greiner, J. Pommerehne, W. Guss, H. Vestweber, H.Y. Tak, H. Bässler, C. Schmidt, G. Lüssem, B. Schartel, V. Stümpflen, J.H. Wendorff, S. Spiegel, C. Möller, H.W. Spiess, V. Stümpften, J.H. Wendorff, S. Spiegel, C. Möller, H.W. Spiess, *Synth. Met*. **1996**, *82*, 1.

[268] J. Vandenbergh, B. Conings, S. Bertho, J. Kesters, D. Spoltore, S. Esiner, J. Zhao, G. Van Assche, M.M. Wienk, W. Maes, L. Lutsen, B. Van Mele, R.A.J. Janssen, J. Manca, D.J.M. Vanderzande, *Macromolecules*. **2011**, *44*, 8470.

[269] R. Kroon, R. Gehlhaar, T.T. Steckler, P. Henriksson, C. Müller, J. Bergqvist, A. Hadipour, P. Heremans, M.R. Andersson, *Sol. Energy Mater. Sol. Cells*. **2012**, *105*, 280.

[270] J. Mun, G.J.N. Wang, J.Y. Oh, T. Katsumata, F.L. Lee, J. Kang, H.C. Wu, F. Lissel, S. Rondeau-Gagné, J.B.H. Tok, Z. Bao, *Adv. Funct. Mater.* **2018**, *1804222*, 1.

[271] G.-J.N. Wang, F. Molina-Lopez, H. Zhang, J. Xu, H.-C. Wu, J. Lopez, L. Shaw, J. Mun, Q. Zhang, S. Wang, A. Ehrlich, Z. Bao, *Macromolecules*. **2018**, *51*, 4976.

[272] H.K. Reimschuessel, *J. Polym. Sci. Polym. Chem. Ed.* **1979**, *17*, 2447.

[273] T.G. Fox, *Bull. Am. Phys. Soc.* **1956**, *1*, 123.

[274] V. Ho, B.W. Boudouris, R.A. Segalman, *Macromolecules*. **2010**, *43*, 7895.

[275] V. Causin, C. Marega, A. Marigo, L. Valentini, J.M. Kenny, *Macromolecules*. **2005**, *38*, 409.

[276] T. Lei, J.-Y. Wang, J. Pei, *Chem. Mater.* **2014**, *26*, 594.

[277] M.U. Ocheje, M. Selivanova, S. Zhang, T.H. Van Nguyen, B.P. Charron, C.-H. Chuang, Y.-H. Cheng, B. Billet, S. Noori, Y.-C. Chiu, X. Gu, S. Rondeau-Gagné, *Polym. Chem.* **2018**, *9*, 5531.

[278] M.U. Ocheje, B.P. Charron, Y.-H. Cheng, C.-H. Chuang, A. Soldera, Y.-C. Chiu, S. Rondeau-Gagné, *Macromolecules*. **2018**, *51*, 1336.

[279] M.U. Ocheje, B.P. Charron, A. Nyayachavadi, S. Rondeau-Gagné, *Flex. Print. Electron.* **2017**, *2*, 43002.

[280] C.P. Radano, O.A. Scherman, N. Stingelin-Stutzmann, C. Müller, D.W. Breiby, P. Smith, R.A.J. Janssen, E.W. Meijer, *J. Am. Chem. Soc.* **2005**, *127*, 12502.

[281] C. Müller, S. Goffri, D.W. Breiby, J.W. Andreasen, H.D. Chanzy, R.A.J. Janssen, M.M. Nielsen, C.P. Radano, H. Sirringhaus, P. Smith, N. Stingelin-Stutzmann, *Adv. Funct. Mater.* **2007**, *17*, 2674.

[282] C. Müller, C.P. Radano, P. Smith, N. Stingelin-Stutzmann, *Polymer.* **2008**, *49*, 3973.

[283] T. Lei, M. Guan, J. Liu, H.-C. Lin, R. Pfattner, L. Shaw, A.F. McGuire, T.-C. Huang, L. Shao, K.-T. Cheng, J.B.-H. Tok, Z. Bao, *Proc. Natl. Acad. Sci.* **2017**, *114*, 5107.

[284] F. Sugiyama, A.T. Kleinschmidt, L. V. Kayser, M.A. Alkhadra, J.M.-H. Wan, A.S.-C. Chiang, D. Rodriquez, S.E. Root, S. Savagatrup, D.J. Lipomi, *Macromolecules*. **2018**, *51*, 5944.

[285] K.F. Freed, *J. Chem. Phys.* **2003**, *119*, 5730.

[286] W.-S. Xu, J.F. Douglas, K.F. Freed, *J. Chem. Phys.* **2016**, *145*, 234509.

[287] W.-S. Xu, K.F. Freed, *Macromolecules*. **2015**, *48*, 2333.

[288] J. Dudowicz, K.F. Freed, J.F. Douglas, *J. Phys. Chem. B.* **2005**, *109*, 21350.

[289] J. Dudowicz, K.F. Freed, J.F. Douglas, *J. Chem. Phys.* **2005**, *123*, 111102.

[290] J. Dudowicz, K.F. Freed, J.F. Douglas, *J. Chem. Phys.* **2006**, *124*, 64901.

[291] J. Dudowicz, K.F. Freed, J.F. Douglas, *Adv. Chem. Phys.* **2007**,.

[292] E.B. Stukalin, J.F. Douglas, K.F. Freed, *J. Chem. Phys.* **2009**, *131*, 114905.

[293] E.B. Stukalin, J.F. Douglas, K.F. Freed, *J. Chem. Phys.* **2010**, *132*, 84504.

[294] J. Dudowicz, J.F. Douglas, K.F. Freed, *J. Chem. Phys.* **2014**, *141*, 234903.

[295] K.F. Freed, *J. Chem. Phys.* **2015**, *143*, 51102.

[296] S. Mirigian, K.S. Schweizer, *Macromolecules*. **2015**, *48*, 1901.

[297] S. Mirigian, K.S. Schweizer, *J. Chem. Phys.* **2014**, *141*, 161103.

[298] S. Mirigian, K.S. Schweizer, *J. Chem. Phys.* **2015**, *143*, 244705.

[299] S.-J. Xie, K.S. Schweizer, *Macromolecules*. **2016**, *49*, 9655.

[300] S. Mirigian, K.S. Schweizer, *J. Chem. Phys.* **2017**, *146*, 203301.

[301] A.D. Phan, K.S. Schweizer, *Macromolecules*. **2018**, *51*, 6063.

[302] S. Peter, H. Meyer, J. Baschnagel, *J. Polym. Sci. Part B Polym. Phys.* **2006**, *44*, 2951.

[303] S. Peter, H. Meyer, J. Baschnagel, R. Seemann, *J. Phys. Condens. Matter*. **2007**, *19*, 205119.

[304] R.J. Lang, D.S. Simmons, *Macromolecules*. **2013**, *46*, 9818.

[305] D.S. Simmons, *Macromol. Chem. Phys.* **2016**, *217*, 137.

[306] T.E. Gartner, A. Jayaraman, *Macromolecules*. **2019**,.

[307] F.L. Lee, A. Barati Farimani, K.L. Gu, H. Yan, M.F. Toney, Z. Bao, V.S. Pande, *J. Phys. Chem. Lett*. **2017**, *8*, 5479.

[308] D.R. Reid, N.E. Jackson, A.J. Bourque, C.R. Snyder, R.L. Jones, J.J. de Pablo, *J. Phys. Chem. Lett*. **2018**, *9*, 4802.

[309] R. Alessandri, J.J. Uusitalo, A.H. de Vries, R.W.A. Havenith, S.J. Marrink, *J. Am. Chem. Soc.* **2017**, *139*, 3697.

[310] W. Zhang, E.D. Gomez, S.T. Milner, *Macromolecules*. **2015**, *48*, 1454.

[311] C. Caddeo, A. Mattoni, *Macromolecules*. **2013**, *46*, 8003.

[312] M. Yoneya, S. Matsuoka, J. Tsutsumi, T. Hasegawa, *J. Mater. Chem. C*. **2017**, *5*, 9602.

[313] O. Alexiadis, V.G. Mavrantzas, *Macromolecules*. **2013**, *46*, 2450.

[314] S.E. Root, S. Savagatrup, C.J. Pais, G. Arya, D.J. Lipomi, *Macromolecules*. **2016**, *49*, 2886.

[315] L.C.E. Struik, *Polym. Eng. Sci.* **1977**, *17*, 165.

[316] L.C.E. Struik, *Physical aging in amorphous polymers and other materials,* Elsevier Scientific Pub. Co., **1978**.

[317] I.M. Hodge, *Science.* **1995**, *267*, 1945.

[318] J.M. Hutchinson, *Prog. Polym. Sci.* **1995**, *20*, 703.

[319] S.L. Simon, *Encycl. Polym. Sci. Technol.* **2001**,.

[320] G.B. McKenna, *Physical Aging in Glasses and Composites*, in: K. V Pochiraju, G.P. Tandon, G.A. Schoeppner (Eds.), *Long-Term Durability of Polymeric Matrix Composites*, Springer, Boston, MA, **2012**.

[321] A.J. Kovacs, Transition vitreuse dans les polymères amorphes. Etude phénoménologique BT - Fortschritte Der Hochpolymeren-Forschung, in: Springer Berlin Heidelberg, Berlin,

Heidelberg, **1964**.

[322] I. Echeverria, P.-C. Su, S.L. Simon, D.J. Plazek, *J. Polym. Sci. Part B Polym. Phys.* **1995**, *33*, 2457.

[323] J. Zhao, G.B. McKenna, *J. Chem. Phys.* **2012**, *136*, 154901.

[324] P.A. O'Connell, G.B. McKenna, *J. Chem. Phys.* **1999**, *110*, 11054.

[325] J. Zhao, S.L. Simon, G.B. McKenna, *Nat. Commun.* **2013**, *4*, 1783.

[326] D. Cangialosi, V.M. Boucher, A. Alegría, J. Colmenero, *Soft Matter*. **2013**, *9*, 8619.

[327] D. Cangialosi, *Encycl. Polym. Sci. Technol.* **2018**,.

[328] J.E. Pye, K.A. Rohald, E.A. Baker, C.B. Roth, *Macromolecules*. **2010**, *43*, 8296.

[329] P.H. Pfromm, W.J. Koros, *Polymer*. **1995**, *36*, 2379.

[330] M.S. McCaig, D.R. Paul, *Polymer*. **2000**, *41*, 629.

[331] M.S. McCaig, D.R. Paul, J.W. Barlow, *Polymer*. **2000**, *41*, 639.

[332] Y. Huang, D.R. Paul, *Macromolecules*. **2005**, *38*, 10148.

[333] Y. Huang, D.R. Paul, *Macromolecules*. **2006**, *39*, 1554.

[334] Y. Huang, X. Wang, D.R. Paul, *J. Memb. Sci.* **2006**, *277*, 219.

[335] R.D. Priestley, L.J. Broadbelt, J.M. Torkelson, *Macromolecules*. **2005**, *38*, 654.

[336] V.M. Boucher, D. Cangialosi, A. Alegría, J. Colmenero, *Macromolecules*. **2012**, *45*, 5296.

[337] B. Frieberg, E. Glynos, P.F. Green, *Phys. Rev. Lett.* **2012**, *108*, 268304.

[338] J.E. Pye, C.B. Roth, *Macromolecules*. **2013**, *46*, 9455.

[339] Q. Tang, W. Hu, S. Napolitano, *Phys. Rev. Lett.* **2014**, *112*, 148306.

[340] H. Yoon, G.B. McKenna, *Sci. Adv.* **2018**, *4*, eaau5423.

[341] R.D. Priestley, *Soft Matter*. **2009**, *5*, 919.

[342] S. Kawana, R.A.L. Jones, *Eur. Phys. J. E*. **2003**, *10*, 223.

[343] R.D. Priestley, C.J. Ellison, L.J. Broadbelt, J.M. Torkelson, *Science*. **2005**, *309*, 456.

[344] N. Van den Brande, G. Van Assche, B. Van Mele, *Polymer*. **2016**, *83*, 59.

[345] S. Bertho, I. Haeldermans, A. Swinnen, W. Moons, T. Martens, L. Lutsen, D. Vanderzande, J. Manca, A. Senes, A. Bonfiglio, *Sol. Energy Mater. Sol. Cells*. **2007**, *91*, 385.

[346] K. Vandewal, A. Gadisa, W.D. Oosterbaan, S. Bertho, F. Banishoeib, I. Van Severen, L. Lutsen, T.J. Cleij, D. Vanderzande, J. V Manca, *Adv. Funct. Mater.* **2008**, *18*, 2064.

[347] H. Sirringhaus, *Adv. Mater.* **2005**, *17*, 2411.

[348] A. Salleo, *Mater. Today*. **2007**, *10*, 38.

[349] V. Coropceanu, J. Cornil, D.A. da Silva Filho, Y. Olivier, R. Silbey, J.-L. Brédas, *Chem. Rev*. **2007**, *107*, 926.

[350] H. Sirringhaus, *Adv. Mater.* **2009**, *21*, 3859.

[351] Y. Li, W.K. Tatum, J.W. Onorato, S.D. Barajas, Y.Y. Yang, C.K. Luscombe, *Polym. Chem*. **2017**, *8*, 5185.

[352] P. Ehrenreich, D. Proepper, A. Graf, S. Jores, A. V Boris, L. Schmidt-Mende, *Phys. Rev. B.* **2017**, *96*, 195204.

[353] H. Sirringhaus, M. Bird, N. Zhao, *Adv. Mater.* **2010**, *22*, 3893.

[354] D. Venkateshvaran, M. Nikolka, A. Sadhanala, V. Lemaur, M. Zelazny, M. Kepa, M. Hurhangee, A.J. Kronemeijer, V. Pecunia, I. Nasrallah, I. Romanov, K. Broch, I. McCulloch, D. Emin, Y. Olivier, J. Cornil, D. Beljonne, H. Sirringhaus, *Nature*. **2014**, *515*, 384.

[355] J.J. Brondijk, W.S.C. Roelofs, S.G.J. Mathijssen, A. Shehu, T. Cramer, F. Biscarini, P.W.M. Blom, D.M. de Leeuw, *Phys. Rev. Lett*. **2012**, *109*, 56601.

[356] A. Gumyusenge, D.T. Tran, X. Luo, G.M. Pitch, Y. Zhao, K.A. Jenkins, T.J. Dunn, A.L. Ayzner, B.M. Savoie, J. Mei, *Science*. **2018**, *362*, 1131.

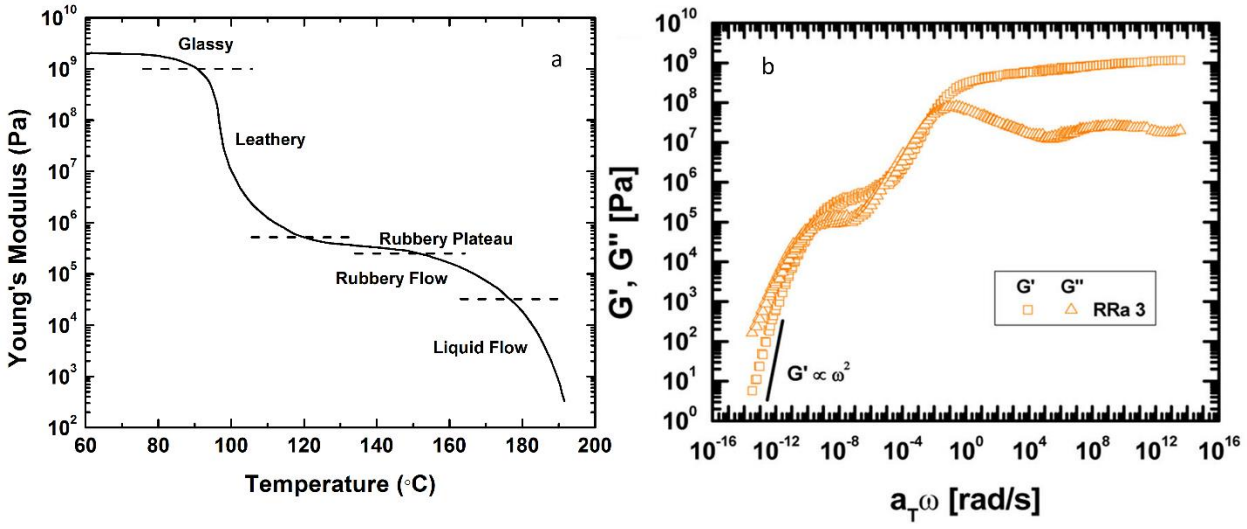

Figure 1. (a). Young's modulus as a function of temperature for a typical amorphous polymer. A high molecular weight polystyrene is shown here. Five different regions of viscoelastic behavior are shown. Adapted with permission.[24] Copyright 1965 John Wiley & Sons, Inc. (b) Dynamic shear moduli for a regiorandom poly(3-hexylthiophene) (P3HT) (weight average molecular weight of 16.7 kg/mol and PDI of 1.15) at reference temperature of 0 °C.[25] Adapted with permission.[25] Copyright 2017 American Chemistry Society.

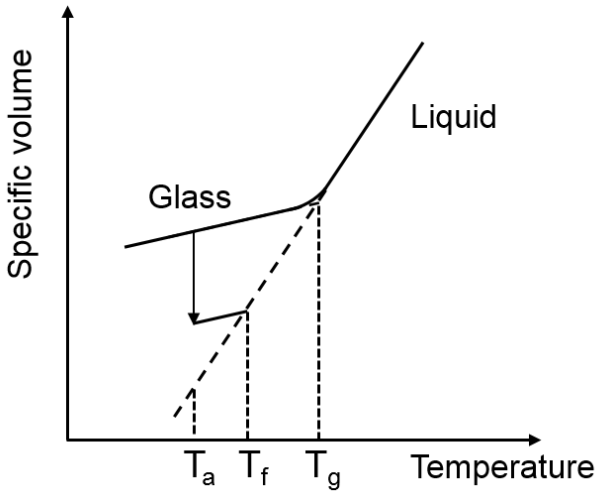

Figure 2. The schematic of temperature dependence of specific volume for a typical amorphous polymer as an illustration. The specific volume follows liquid line (or equilibrium line) when temperature decreases until below certain temperature, the T_g, it departs and follows the nonequilibrium glass line. At a temperature T_a, which is below T_g, the polymer is in the glassy state and the specific volume has the tendency to reduce towards the equilibrium (as indicated by the arrow). This process is referred to as physical aging, or also known as structure recovery. When

this aged sample is heated up, it follows a line parallel to the glass line and intersects with the equilibrium line at the fictive temperature T_f.

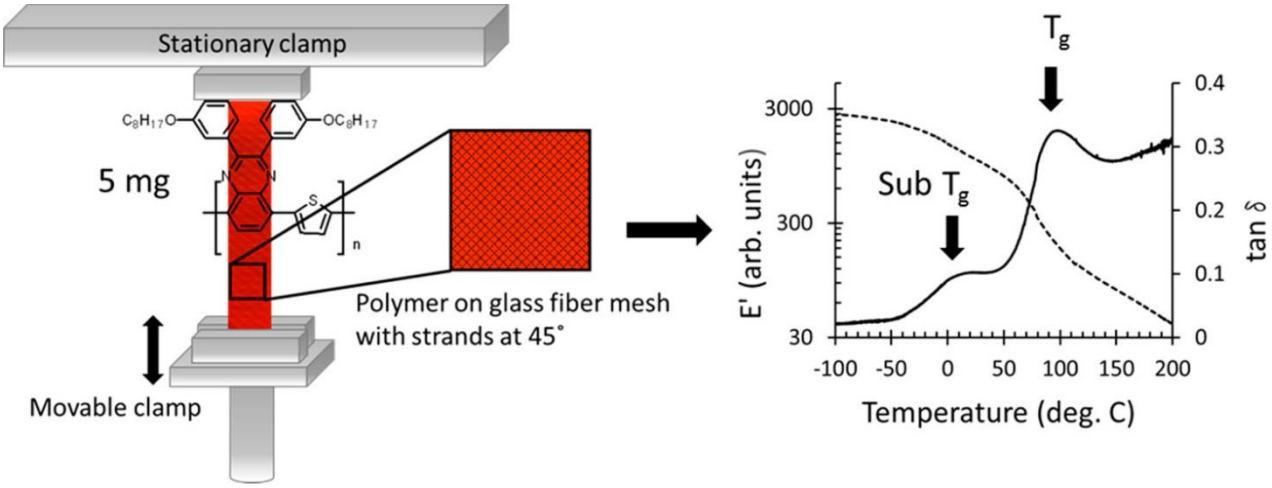

Figure 3. The schematic representation of thin film DMA instrument set-up for measuring conjugated polymers, which is drop-coated onto the glass fiber from the solution. The peaks in the resultant tan δ response correspond to the glass transition and sub- T_g transitions.[126] Because of unspecified sample geometry, absolute moduli cannot be acquired. Adapted with permission.[126] Copyright 2017 American Chemistry Society.

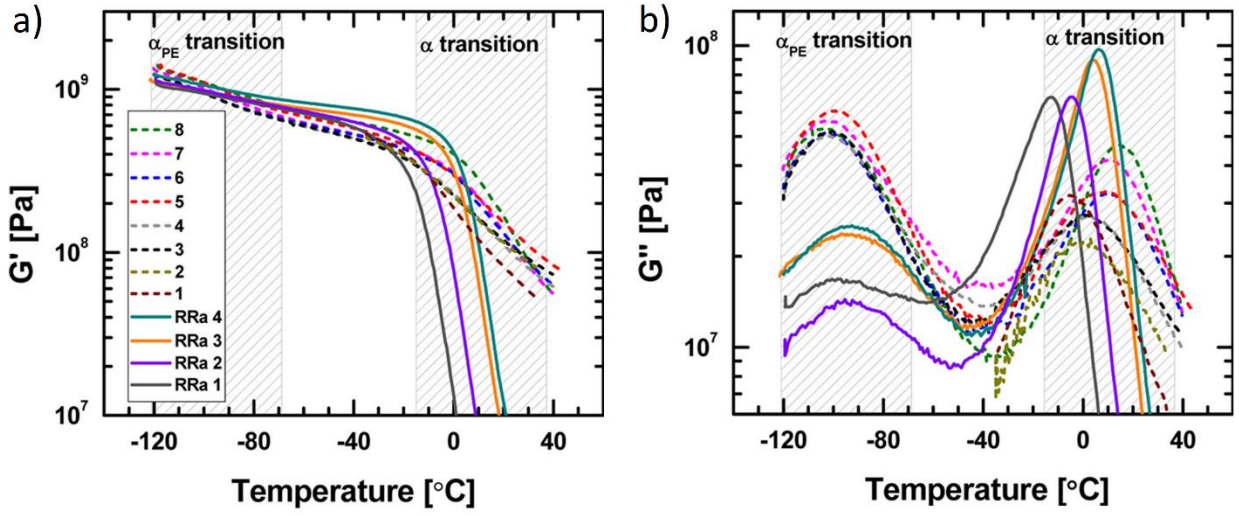

Figure 4. The dynamic moduli data (a). storage modulus (G') and (b). loss modulus (G'') for eight regioregular and four regiorandom P3HTs measured from temperature ramp with a fixed frequency of 10 rad/s, 0.1% strain amplitude and heating rate of 5 °C /min.[25] The T_gs of backbone (α-process) and side chain (α_{PE}-process) are determined from the two peaks in G''. Adapted with permission.[25] Copyright 2017 American Chemistry Society.

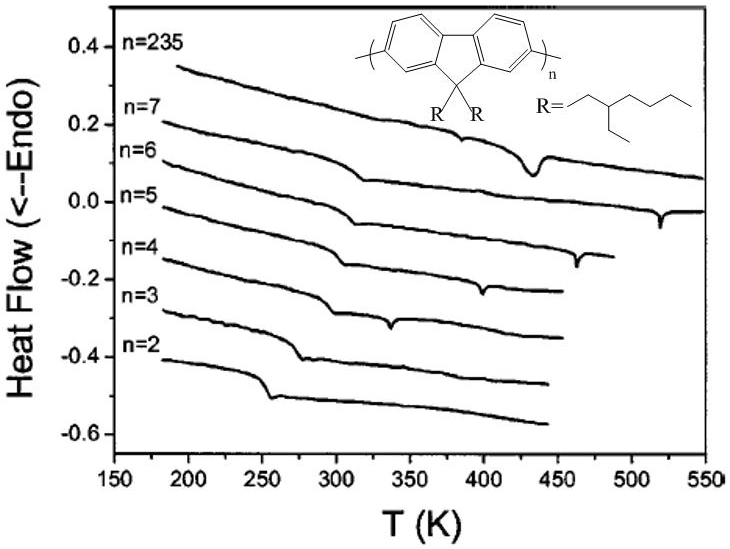

Figure 5. The DSC traces from second heating scan for the oligofluorenes and the polyfluorene.[122] The heating/cooling rate is 10 K/min. The monomer structure is depicted in the plot. The T_g can be readily determined for oligofluorenes, which is varied from 253 K for dimer to 316 K for heptamer. However, polyfluorene does not exhibit a clear glass transition. Adopted with permission.[122] Copyright 2004 AIP Publishing.

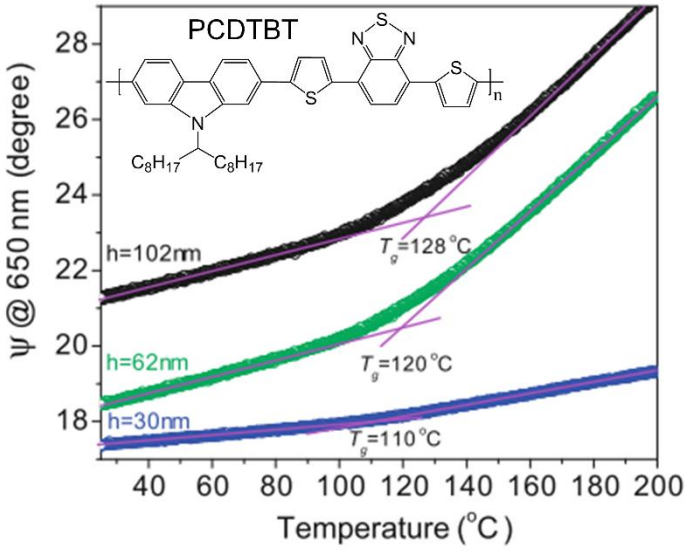

Figure 6. The temperature dependence of ellipsometric angle Ψ investigated with ellipsometry for poly[N-9'-heptadecanyl-2,7-carbazole-alt-5,5-(4',7'-di-2-thienyl-2',1',3'-benzothiadiazole)] (PCDTBT) ultrathin films supported on Si/SiO_x substrate, as indicated in the figure legend.[197] The T_g for each film thickness is determined from the intersection of two linear fits. A T_g depression with film thickness is readily observed. Adapted with permission.[197] Copyright 2012, The Authors.

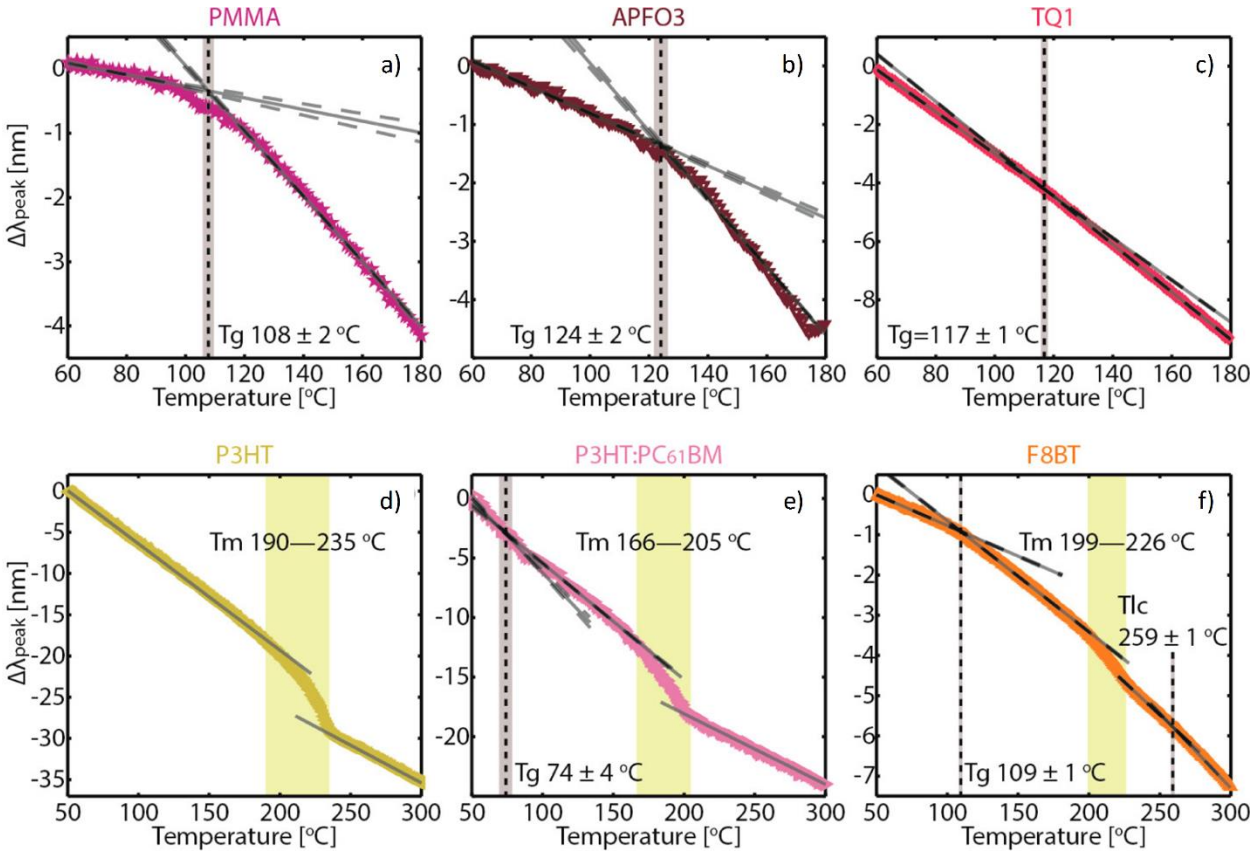

Figure 7. Thermal transitions (glass transition T_g, melting T_m, and nematic-isotropic transition T_{lc}) in (a) polymethyl methacrylate (PMMA), (b) poly(2,7-(9,9-dioctylfluorene)-alt-5,5-(4',7'-di-2-thienyl-2',1',3'-benzothiadiazole)) (APFO3), (c) poly[[2,3-bis(3-octyloxyphenyl)-5,8-quinoxalinediyl]-2,5-thiophenediyl] (TQ1), (d) poly(3-hexylthiophene) (P3HT), (e) poly(3-hexylthiophene): [6.6]-phenyl C61 butyric acid methyl ester (P3HT:$PC_{61}BM$), and (f) poly(9,9-dioctylfluorene-alt-benzothiadiazole) (F8BT) determined from the plasmonic nanospectroscpy measurements.[204] Adapted with permission.[204] Copyright 2017 American Chemical Society.

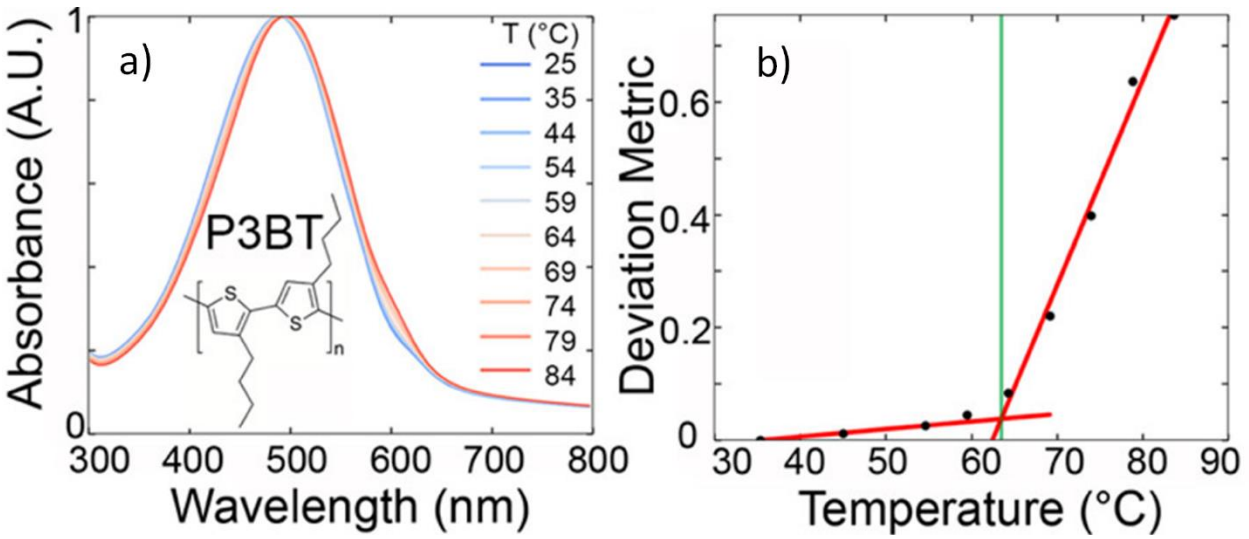

Figure 8. The (a) UV-vis absorption spectra and (b) deviation metric as a function of annealing temperature for P3BT thin film.[206] Adapted with permission.[206] Copyright 2017 American Chemical Society.

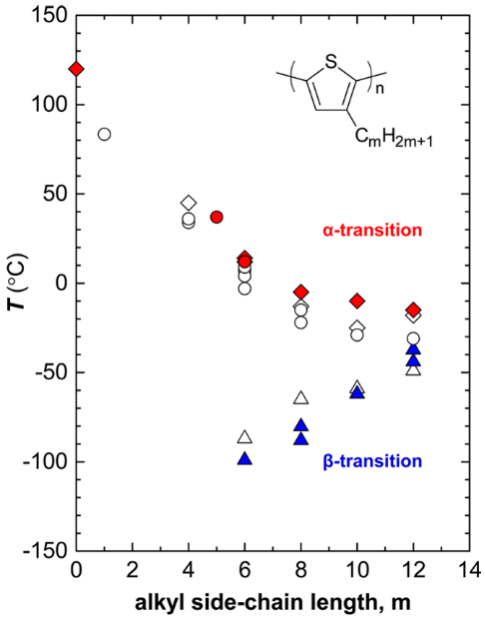

Figure 9. Backbone T_g (α-transition) and side-chain T_g (β-transition) of poly(3-alkylthiophene)s (P3AT)s with various linear alkyl side-chain lengths.[207] The filled symbols and open symbols are T_gs for regioregular and regiorandom (P3AT)s, respectively. Adapted with permission.[207] Copyright 2015 American Chemical Society.

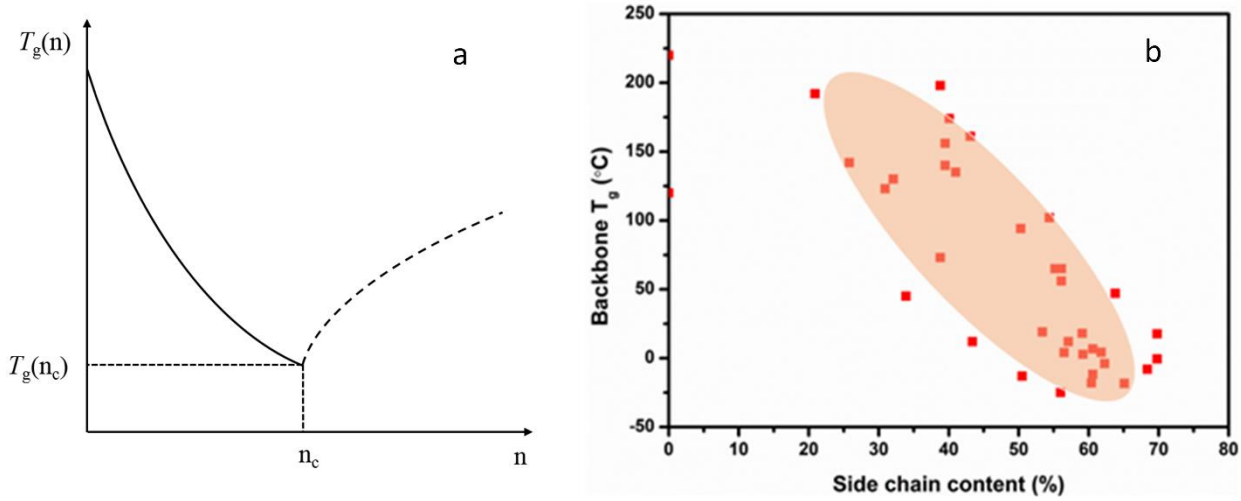

Figure 10. (a) A schematic representation of the T_g varying with the number of side chain methylene groups.[272] Adapted with permission.[272] Copyright 2003 John Wiley and Sons. (b) Summary of backbone T_g as a function of the content of the side chain groups for conjugated polymers.

Table 1. The summary of advantages and disadvantages for the experimental techniques when measuring the T_g for conjugated polymers

Experimental Techniques	Advantages	Disadvantages
Broadband dielectric spectroscopy	a. Low mass requirement b. Broad range of frequency c. High sensitivity	Dielectric relaxation response can be masked by the low-frequency conductivity slope due to electric conductivity
Dynamic mechanical analysis (Specifically for technique using polymer in a pocket or on thin substrate)	a. Low mass requirement b. High sensitivity c. Detect T_g for conjugated polymers with high crystallinity	a. Cannot obtain absolute moduli because of unspecified sample geometry b. Possibly misinterpret data when multiple thermal transitions are present c. Only measure bulk T_g
Advanced rheometry	a. Able to obtain absolute moduli b. Can identify different thermal transitions c. High sensitivity	a. Relatively large mass requirement b. Only measure bulk T_g
Differential scanning calorimetry	a. Broad temperature range b. Can identify different thermal transitions c. Simple experiment set-up	a. can not measure nanoscale film samples Relatively low cooling rate compared with flash DSC and AC-Chip calorimetry b. T_g may not be detectable with small heat capacity change results from 1).

		Sample crystallization during cooling, 2). Incompletely removed thermal history due to high crystallinity and low degradation temperature
Fast Scan (Flash) DSC	a. Low mass requirement b. Broad temperature range c. Fast cooling rate to avoid crystallization	a.May not be able to detect T_g if the thermal history cannot be completely removed due to high crystallinity and low degradation temperature b.Film-substrate interaction affects T_g
AC-chip calorimetry	a. Low mass requirement b. Broad temperature range c. High sensitivity of ~ 50 pJ/K d. Able to detect T_g for conjugated polymers with high crystallinity	a. Relatively limited access b.Film-substrate interaction affects T_g
Ellipsometry	a. Low mass requirement b. Measure thin film T_g	a. The donor-acceptor conjugated polymers with a large range of absorption spectrum may interfere with laser b. Film-substrate interaction affects T_g
Plasmonic nanospectroscopy	Low mass requirement	a. Lack of the evidence of the application on conjugated polymers with T_g below room temperature b. Film-substrate interaction affects T_g
UV-vis spectroscopy with temperature stage	a. Low mass requirement b. Easy access to instrument	a. Not broadly applicable to all semicrystalline conjugated polymers b. Lack of the evidence of the application on conjugated polymers with T_g below room temperature

Table 2. T_g of thiophene-based polymers

Polymer	Structure	T_g [°C]	Side chain T_g [°C]	Test Method	Side chain content [%]	M_n [kg/mol]	PDI	Ref.
PT	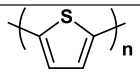	120		DMA	0			[215]
P3BT		45		DMA	33.9	17	4.1	[129]

	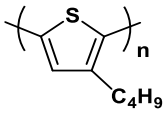	60		UV-Vis				[206]
P3HT	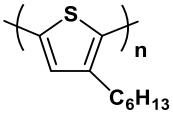	12	-87	DMA	43.4	10	2.1	[129]
P3OT	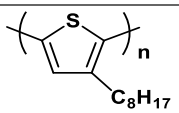	-13	-65	DMA	50.5	21	2.6	[129]
P3DT	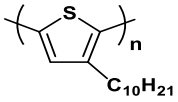	-25	-59	DMA	56.0			[129]
P3DDT	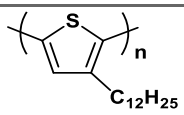	-18	-49	DMA	60.4			[129]
P3EHT	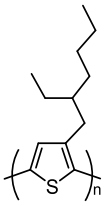	24		DMA (glass fiber)	50.5	24	1.8	[217]
PBTTT	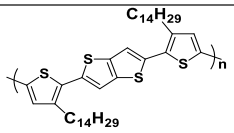	102		UV-Vis	54.4	>12	1.8	[206]

Table 3. T_g of fluorene-based polymers

Polymer	Structure	T_g [°C]	Test Method	Side chain content [%]	M_n [kg/mol]	PDI	Ref.
F6	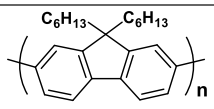	94	DSC	50.3	17	4.1	[223]
		103	DSC		16	2.8	[233]
F8	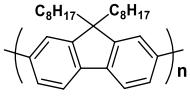	65	DSC	56.1	10	2.1	[234]
		72	DSC		24	4.4	[223]
		50~63	Ellipsometry				[195]

F12	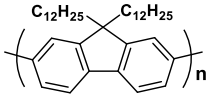	47	DSC	63.8	21	2.6	[223]
F2/6	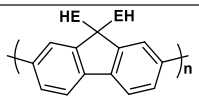	56	DSC	56.1	98	2.3	[122]
		80	DSC		83	2.0	[235]
F82T	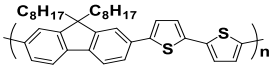	73	DSC	38.8	15	3.0	[224]
		80	DSC		15	2.1	[225]
		108	DSC		36	3.1	[226]
F8BT	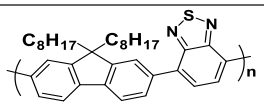	135	DSC	41.0	188	2.2	[227]
		104	UV-Vis				[206]
APFO-3 (PFTBT)	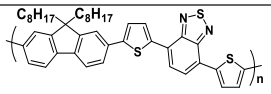	123	DSC	30.9	38	1.8	[229]
		133	DSC		9.3	3.9	[230]
APFO-18	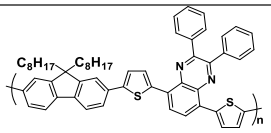	142	DSC	25.8	8	2.3	[231]
APFO-Green9	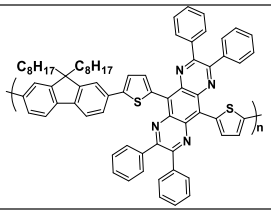	177	Ellipsometry	20.9	10	1.9	[200]
		192	DSC		10	1.9	[231]
TFB-B	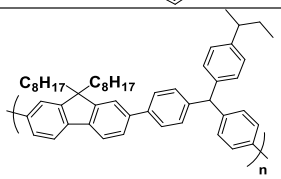	140	Ellipsometry	39.5	57	2.1	[201]
TFB-L	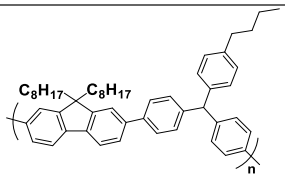	156	DSC	39.5			[232]

Table 4. T_g of bridged and fused ring polymers

Polymer	Structure	T_g [°C]	Test Method	Side chain content [%]	M_n [kg/mol]	PDI	Ref.

PIDTBTD	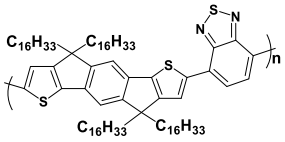	17.6	DSC	69.8	15	1.7	[241]
PIDTTPD	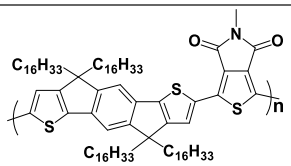	-0.6	DSC	69.8	14	1.6	[241]
PIDTBPD	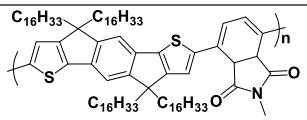	-8.1	DSC	68.4	15	1.7	[241]
PCDTBT	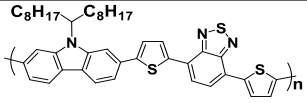	130	Ellipsometry	32.1	18.7	1.57	[197]
		126	DMA		20-100		[126]
		129	DSC		13.7	3.7	[230]
PTB7-Th	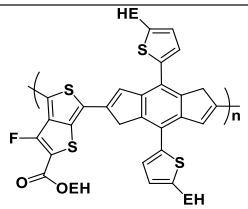	138	DMA	38.4			[242]
PTB7	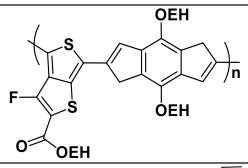	127	MD	51.6			[243]
PCPDTBT	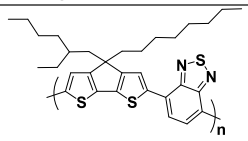	174	Rapid heat-cool calorimetry (RHC)	40.1	26	3.2	[244]
PCPDTBT-OH	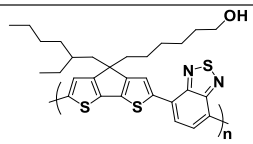	198	RHC	38.8	13	2.5	[244]
PCPDTBT-Ester	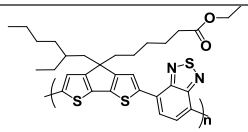	161	RHC	43.1	46	1.7	[244]
PDTSTPD-C8		106	UV-Vis	47.8			[206]

	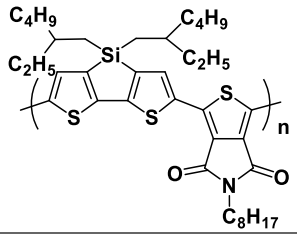	109	DSC		31	[245]
		107	Molecular dynamics (MD)			[243]
PDTSTPD-C6	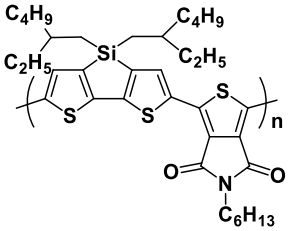	109	DSC	47.6	26	[245]
PDTSTPD-C4	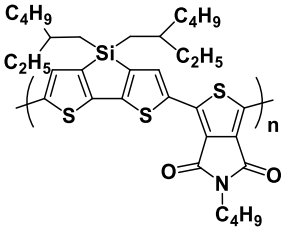	109	DSC	46.4	25	[245]

Table 5. T_g of diketopyrrolopyrrole (DPP)-based and isoindigo-based polymers

Polymer	Structure	T_g [°C]	Side chain T_g [°C]	Test Method	Side chain content [%]	M_n [kg/mol]	PDI	Ref.
P(DPPT)	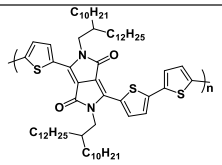	-4.0	-54.3	DMA (glass fiber)	62.3	47	2.83	[256]
		-11		AC-chip calorimetry				
P(DPPT2)	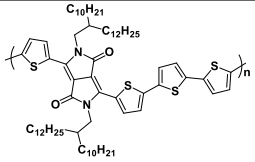	12.0	-51.9	DMA (glass fiber)	57.1	44	3.96	[256]
		17		AC-chip calorimetry				
P(DPPT3)	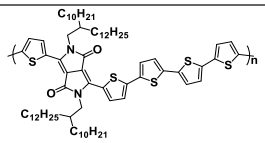	19.0	-47.9	DMA (glass fiber)	53.4	27	3.18	[256]
		19		AC-chip calorimetry				
P(DPPTT)		2.8	-53.0	DMA (glass fiber)	59.2	51	3.62	[256]

	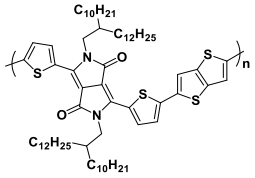	3.5		AC-chip calorimetry				
P(DPPTT)-C8C10	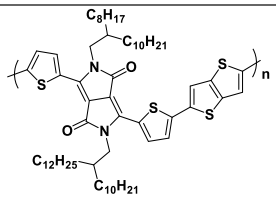	131 (thick film)	-64	AC-chip calorimetry	57.1	27	3.7	[10]
		87 (thin film)	-62					
		64 (nano fiber)	-63					
P(DPPTTT)	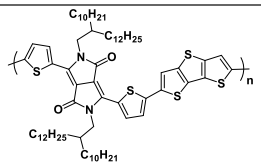	4.1	-52.5	DMA (glass fiber)	56.5	26	3.69	[256]
		22		AC-chip calorimetry				
P(DPPTVT)	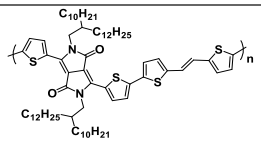	24.5		AC-chip calorimetry	56.7	46.9	2.1	[165]
P(DPPT3-C8)	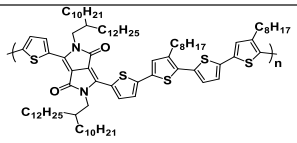	-11.8	-51.5	DMA (glass fiber)	60.6			[256]
C16-PTDPPTFT4	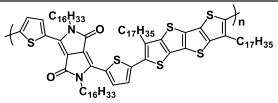	4.3		DMA (Kapton film)	61.8			[208]
C8C10-PTDPPTFT4	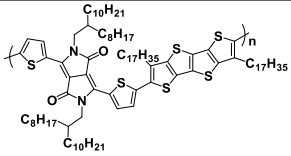		-48	DMA (Kapton film)				[208]
C8C10-PT2DPPT2FT4	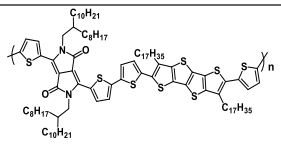		-48	DMA (Kapton film)				[208]
PTBTD-2DT	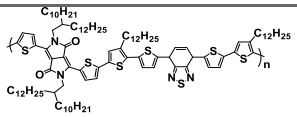	32		DSC	56.3	28	2.5	[261]

C6C10DPPT-TT	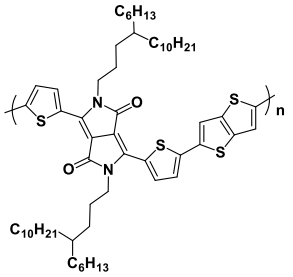		-56	DSC		45	3.1	[262]
C8C10DPPT-TT	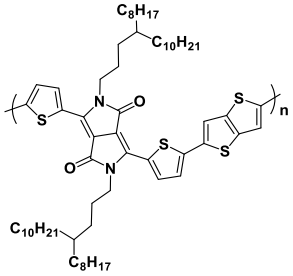		-58	DSC		49	3.2	[262]
C10C10DPPT-TT	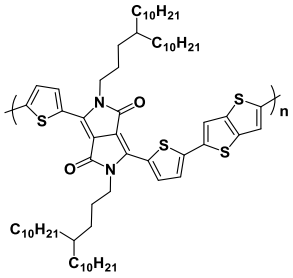		-57	DSC		53	3.1	[262]
PiI2T	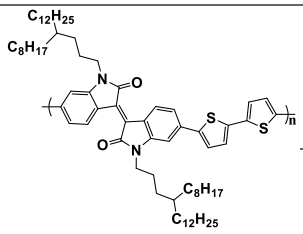	43	-27	DMA (Kapton film)	59.9	33	3.4	[125]
			-37	DSC				
			-82	AC-chip calorimetry				

Table 6. T_g of other conjugated polymers

Polymer	Structure	T_g [°C]	Test Method	Side chain content [%]	M_n [kg/mol]	PDI	Ref.
PPV	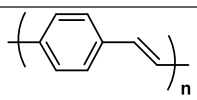	220	DMA	0			[267]

MDMO-PPV	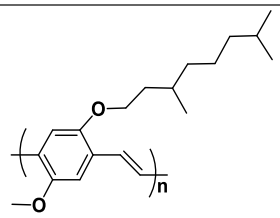	18	DSC	59.1	106	16.7	[188]
		50	DSC		123	3.2	[265]
MEH-PPV	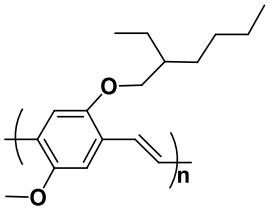	65	DSC	55.2	400	1.6	[264]
		66	DSC		45	3.2	[265]
MPE-PPV	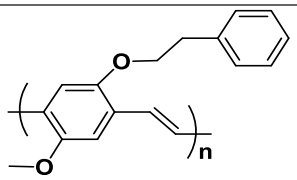	111	DSC		53	2.3	[268]
		111	DSC		65	3.9	[188]
TQ1	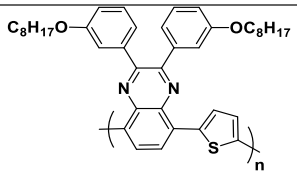	100	DSC	39.8	46	2.6	[269]
		95	DMA		132		[126]
		102	MD				[243]
TQ-N	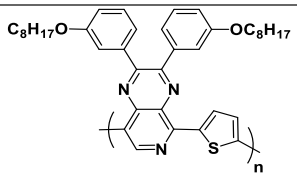	46	DSC				[269]
TQ-8A	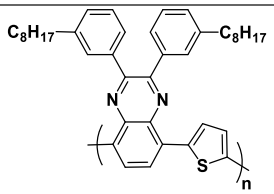	96	DSC				[269]
TQ-F	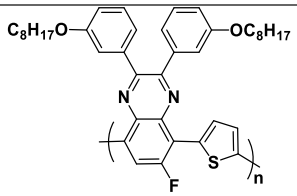	48	DSC				[269]
PA3T-BC2-C10C12	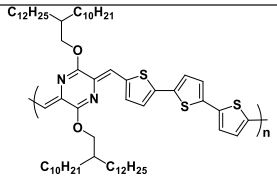	-18.4	DMA	65.1			[256]

PA4T-BC2-C10C12	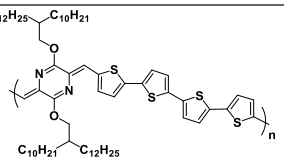	6.7	DMA	60.6		[256]

Table 7. Experimental and predicted T_g for a series of DPP polymers.

Polymer	Structure	Predicted T_g (°C)*	Experimental T_g (°C)	Ref.
P(DPPT)	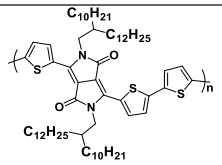		-4.0	[256]
P(DPPT2)	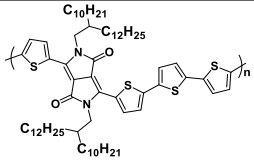	3	12.0	[256]
P(DPPT3)	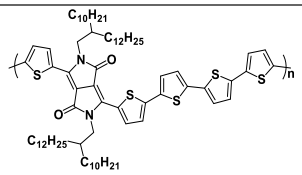	13	19.0	[256]

* The glass transition temperatures have been calculated with the Fox equation using the following values $T_{g,\,P(DPPT)} = -4.0$ °C, $T_{g,\,PT} = 120$ °C.

Table of Contents: This paper reviews the glass transition phenomenon of conjugated polymers. The glass transition temperature data for a broad range of conjugated polymers are compiled and discussed. Empirical design rules are proposed to guide the fine-tune of glass transition in conjugated polymers. The challenges and opportunities in understanding glass transition and connecting it to the end use performance are also discussed.

Key words: Conjugated polymers, Glass transition temperature, Semiconducting materials, Flexible electronics.

*Zhiyuan Qian, Zhiqiang Cao, Luke Galuska, Song Zhang, Xiaodan Gu**

Title: Glass Transition Phenomenon for Conjugated Polymers

ToC figure: